Earth-Science Reviews 112 (2012) 97–114

Contents lists available at SciVerse ScienceDirect

Earth-Science Reviews

journal homepage: www.elsevier.com/locate/earscirev

Sources and characteristics of acoustic emissions from mechanically stressed geologic granular media — A review

Gernot Michlmayr [a,*], Denis Cohen [a,b], Dani Or [a]

[a] *Department of Environmental Sciences, ETH Zurich, Universitätsstrasse 16, 8092 Zürich, Switzerland*
[b] *Department of Geological and Atmospheric Sciences, Iowa State University, 253 Science I, Ames, Iowa 50011, USA*

ARTICLE INFO

Article history:
Received 19 October 2011
Accepted 25 February 2012
Available online 8 March 2012

Keywords:
Acoustic emissions
Geophysics
Granular mechanics
Failure precursors

ABSTRACT

The formation of cracks and emergence of shearing planes and other modes of rapid macroscopic failure in geologic granular media involve numerous grain scale mechanical interactions often generating high frequency (kHz) elastic waves, referred to as acoustic emissions (AE). These acoustic signals have been used primarily for monitoring and characterizing fatigue and progressive failure in engineered systems, with only a few applications concerning geologic granular media reported in the literature. Similar to the monitoring of seismic events preceding an earthquake, AE may offer a means for non-invasive, in-situ, assessment of mechanical precursors associated with imminent landslides or other types of rapid mass movements (debris flows, rock falls, snow avalanches, glacier stick-slip events). Despite diverse applications and potential usefulness, a systematic description of the AE method and its relevance to mechanical processes in Earth sciences is lacking. This review is aimed at providing a sound foundation for linking observed AE with various micro-mechanical failure events in geologic granular materials, not only for monitoring of triggering events preceding mass mobilization, but also as a non-invasive tool in its own right for probing the rich spectrum of mechanical processes at scales ranging from a single grain to a hillslope. We review first studies reporting use of AE for monitoring of failure in various geologic materials, and describe AE generating source mechanisms in mechanically stressed geologic media (e.g., frictional sliding, micro-crackling, particle collisions, rupture of water bridges, etc.) including AE statistical features, such as frequency content and occurrence probabilities. We summarize available AE sensors and measurement principles. The high sampling rates of advanced AE systems enable detection of numerous discrete failure events within a volume and thus provide access to statistical descriptions of progressive collapse of systems with many interacting mechanical elements such as the fiber bundle model (FBM). We highlight intrinsic links between AE characteristics and established statistical models often used in structural engineering and material sciences, and outline potential applications for failure prediction and early-warning using the AE method in combination with the FBM. The biggest challenge to application of the AE method for field applications is strong signal attenuation. We provide an outlook for overcoming such limitations considering emergence of a class of fiber-optic based distributed AE sensors and deployment of acoustic waveguides as part of monitoring networks.

Contents

* Corresponding author.
E-mail addresses: gernot.michlmayr@env.ethz.ch (G. Michlmayr), dcohen@iastate.edu (D. Cohen), dani.or@env.ethz.ch (D. Or).

0012-8252/$ – see front matter
doi:10.1016/j.earscirev.2012.02.009

1. Introduction

Non-invasive characterization of deformation processes and mechanical failures of geologic granular materials is of great interest for applications in engineering, natural hazard mitigation, and material sciences. Mechanically induced elastic waves, often termed acoustic emissions or AE for short, provide a window into grain-scale processes not attainable with traditional monitoring techniques. AE are relatively high frequency (10–1000 kHz), rapid (few milliseconds), small magnitude body waves generated by the abrupt release of stored strain energy from a delimited source region (Lockner, 1993). Crack formation, grain rearrangement, friction between solid surfaces, and other grain-scale motion are typical processes generating AE.

Modern AE acquisition systems are capable of sampling rates exceeding tens of MHz and able to capture a massive number of discrete events emanating from a deforming geologic sample. AE monitoring can therefore complement other mechanical measurements of stress or strain by providing a measure of discrete mechanical interactions as singular events. The monitoring of acoustic emissions activity in engineering applications is routinely used for the assessment of the integrity of key structural elements in civil infrastructure such as bridges (e.g., Shigeishi et al., 2001) or deep excavations (e.g., Young and Martin, 1993) and for testing engineering materials such as concrete (e.g., Labuz et al., 2001) and fiber-reinforced composites used in aerospace or automobile engineering (e.g., Barre and Benzeggagh, 1994). In Earth sciences, AE activity has received considerable attention in the study of rock strength and fracture properties (Lockner, 1993). However, despite over half a century of acoustic emission research on geologic granular materials, the method has not enjoyed widespread application probably owing to the fundamental issues related to signal attenuation in porous media often requiring prohibitively large number of sensors for implementation at practical scales of interest. An array of important issues in granular mechanics could benefit from judicious application of acoustic emission method. For example, grain-scale micro-mechanical interactions resulting in the development of shear zones and localized deformations, grain rearrangements, or formation of force concentrations can potentially produce large numbers of AE whose characteristics and statistics could be used to identify granular deformation events. AE-producing granular interactions also determine how a granular material collapses when external stresses exceed the macroscopic strength of the material (Tordesillas and Behringer, 2009). The capacity of counting discrete events offered by AE data acquisition systems may provide a valuable measurement tool for investigations of progressive failure of granular materials.

Theoretical aspects and applications of AE have been summarized in various textbooks (e.g., Kino, 1987; Grosse and Ohtsu, 2008) and reviews (e.g., Swindlehurst, 1973; Scruby, 1987; Boyd and Varley, 2001). Studies on specific applications of acoustic emissions were published for example on crack formation and propagation in brittle materials (Evans and Linzer, 1977), on brittle rock failure (e.g., by Yamada et al., 1989), concrete (Ohtsu and Watanabe, 2001), or fiber-reinforced resins (Barre and Benzeggagh, 1994). In geosciences Koerner and co-workers have measured AE from soils and sands to assess stability of slopes (Lord and Koerner, 1974, 1975; Koerner et al., 1976, 1977; Huck and Koerner, 1981; Koerner et al., 1981a).

Koerner et al. (1977) also reported tests for the detection of mechanical failure in clayey or silty soils by measuring elastic body waves and have shown empirically that acoustic emissions are generated during failure of different geologic granular materials (see Fig. 1). In the context of landslide hydrological processes, Cadman and Goodman (1967) were among the first to implement the acoustic emission technique as a tool for monitoring slope movement. Rouse et al. (1991) measured significant acoustic emission activity following heavy rainfall events within a slope prone to landslide and attributed it to localized hydromechanical destabilization. In another field study Chichibu et al. (1989) found indication that AE activity increases at the onset of slope deformation induced by heavy rainfalls. Shiotani and Ohtsu (1999) evaluated statistical prediction methods to use AE signals for slope failure early warning. The authors addressed also the issue of strong AE signal attenuation within geologic materials and proposed different design options for waveguides, i.e. low-attenuation structures that help to reduce propagation losses of AE signals. Recent advances in application of acoustic emissions for slope stability detection using waveguides were made by Dixon and co-workers (Dixon et al., 2003; Dixon and Spriggs, 2007). The authors reported measurements of acoustic emissions in combination with steel waveguides in a borehole backfilled with sand or gravel ("active waveguides") in a field site to monitor slope instabilities. Sommerfeld and Gubler (1983) and van Herwijnen and Schweizer (2011b) tested the application of AE for monitoring of a snow avalanche initiation zone and have identified a range of low frequency precursory AE events indicative of imminent avalanche release. Recent developments in AE measurement techniques using optical fiber offer exciting potential for large and distributed earth science applications in terms of monitoring and analyzing progressive mechanical failure (Inaudi and Glisic, 2005; Selker et al., 2006; Iten, 2008; B.J. Wang et al., 2009; Zeni, 2009; Iten, 2011). These applications enable monitoring of strains and AE-induced vibrations at rapid sampling rates (>100 Ksamples/s/m) over several kilometers at sub-meter resolution.

Acoustic emissions were also used for experimental granular physics studies of grain-to-grain or sample scale mechanical interaction. Hidalgo et al. (2002) used acoustic emission signals to study internal force rearrangements in assemblies of glass beads. Gardel et al. (2009) measured rapid force and velocity fluctuations due to grain collisions and frictional interaction with piezoelectric sensors in dense granular flows. Recently Carson et al. (2008, 2009) monitored particle size distribution of powders by acoustic emissions generated

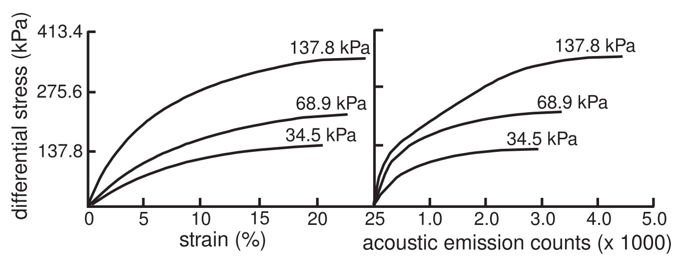

Fig. 1. Results from Koerner et al. (1977) that demonstrate the occurrence of acoustic emissions during shear deformation of soil. The graphs show the stress strain behavior of a clayey silt soil and the corresponding cumulative number of AE events. (Figure modified after Koerner et al., 1977).

by grain-grain or grain-wall collisions. Allan et al. (2010) recorded acoustic emissions at the wall of a mixer vessel during blending of pharmaceutical powders and were able to assign features of the elastic waves to material properties such as grain size or density (for a review of AE applications in chemical engineering processes see Boyd and Varley, 2001). Similar efforts were undertaken by Cody et al. (1996) and by Jiang et al. (2007) to understand random motion of granular material entrained by a gas flow inside a container. Complementary to empirical use of AE measurements, there are strong links between elastic waves produced by failure mechanisms and statistical models of failure such as the fiber bundle model (as e.g. described by Turcotte et al., 2003). Linking frequency–magnitude characteristics of measured acoustic events to the imminence of collapse offers a promising possibility for early warning applications.

Notwithstanding the number of studies addressing occurrence of AE and other forms of elastic waves in granular geologic materials, relatively little is known about mechanisms that generate such acoustic waves. Correspondingly, there is little coherent information regarding characteristics, frequency content, and amplitudes of elastic waves generated by micro-mechanical interactions in granular materials. Additionally the number of acoustic events, their occurrence frequency, and their temporal distribution in mechanically stressed granular material remains an open question. Perhaps the most critical obstacle to the widespread application of acoustic emission method for study and monitoring of mechanical interaction and states of geologic materials is a relatively short propagation distance of acoustic emissions in such media (Koerner et al., 1981b).

Despite several benchmark studies (e.g., Koerner et al., 1977; Rouse et al., 1991; Mair et al., 2007; Gardel et al., 2009; Y. Wang et al., 2009) on acoustic emissions in geologic granular materials, no overarching review has been presented on the topic that summarizes results and knowledge. Hence, the primary goal of this review was to introduce Earth scientists and geoengineers to the field of acoustic emissions and its potential (Section 2). An important objective was to establish links between certain physical processes associated with shear, compression and other forms of mechanical loading of granular media and associated acoustic emissions to capture failure progression. Different micro-mechanical mechanisms that may generate acoustic emissions in geologic materials will be reviewed to quantify number of events, occurrence rates, and intrinsic frequencies (Section 3). Links between acoustic signals and conceptual mechanical models to enable interpretation of measured AE in deterministic and stochastic frameworks will be presented in Section 4. We will present the fiber bundle model as a potential tool for linking progressive failure in granular materials with AE events (Section 5). Finally the use of acoustic emissions for monitoring the imminent failure in field applications will be discussed (Section 6). Advances in rapid and highly resolved AE acquisition systems may provide new insights into micro-mechanical processes associated with stress–strain relationship and thus complement existing geotechnical testing procedures. Additionally, the AE technique offers a promise for early detection of precursor events preceding slope failure which otherwise may appear as an abrupt and erratic event (Dixon et al., 2003; Dixon and Spriggs, 2007).

2. Measurement of acoustic emissions

Acoustic emissions (AE) measurements are motivated by the propensity of certain materials to generate elastic body waves during deformation and abrupt grain-scale mechanical interactions. Intermittent and rapid mechanical perturbations within a body may produce audible sound, as encountered in our daily experience with the crackling sound of paper crumpling, the snapping of timber, or the noise emitted by a metal object during deformation. Capturing acoustic emissions requires the detection of these mechanical (elastic) waves within a body by measurements of small motion at its surface.

Many engineering applications such as material testing of aircraft structural integrity (e.g., Staszewski et al., 2004), monitoring of bridges and other civil structures (e.g., Ohtsu and Watanabe, 2001; Shigeishi et al., 2001), engineering geology (e.g., Zang et al., 1996) or rock mechanics (Lockner, 1993), make use of piezoelectric sensors for measurements of AE. Piezoelectricity is the property of certain materials to generate an electric potential when mechanically strained (Kino, 1987). In an AE sensor, a piezoelectric crystal, often a manufactured ceramic such as lead zirconate titanate, is protected by a wear plate that is in direct contact with the surface of the monitored structure, and transforms incident elastic waves into an analog signal (see Fig. 2). Piezoelectric sensors have become the standard method for capturing and analyzing acoustic emission waves and are commercially available from many manufacturers (e.g., Bruel & Kjaer, Physical Acoustics Corporation, Vallen Systeme, etc.).

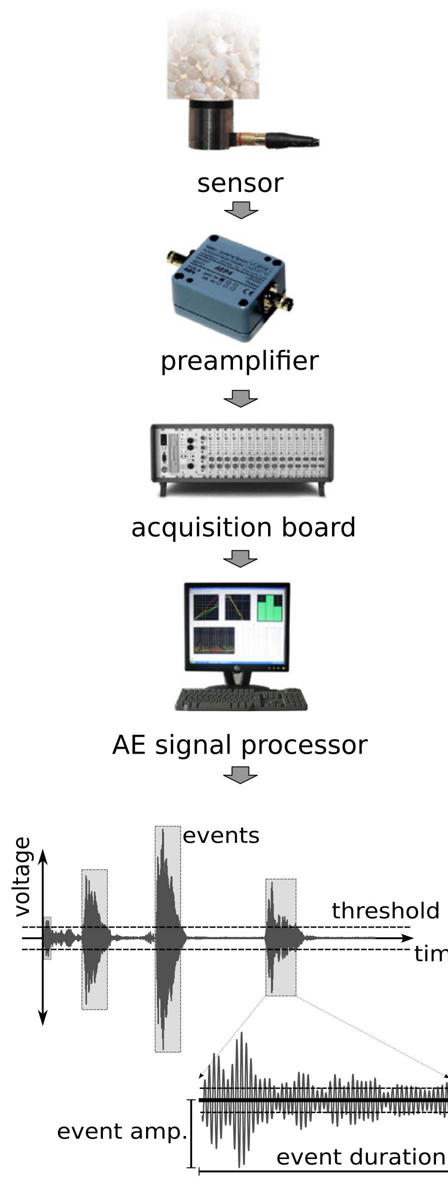

Fig. 2. Principle of the acoustic emission technique: The piezoelectric sensor is in direct contact with the material to be tested. Vibrations at the sensors piezoelectric surface are transformed into a voltage signal that is usually amplified before being transmitted to an acquisition board, where it is converted into digital form. Visualization, data processing and analysis of this signal is done using a conventional PC. The bottom panel illustrates the extraction of AE events from the continuous, transient waveform. Most important event features are shown in the inset.

We may distinguish two types of piezoelectric sensors based on their operating principle: (a) Resonance-type sensors are designed to respond strongly to waves of a certain frequency range corresponding to the sensor resonance spectrum. Such sensors are highly sensitive to acoustic emissions close to their central frequencies. Elastic waves with intrinsic frequencies outside the sensor spectrum are captured with lower sensitivity. Consequently, full waveform analysis of Fourier spectra acquired by such sensors is limited by this inherently biased response. (b) Broadband sensors that are designed to acquire acoustic signals with a uniform response over a wide range of frequencies. Their sensitivity is typically lower, however frequencies captured by the sensor are all represented relatively equally. Piezoelectric AE sensors typically operate in the frequency range from 10 kHz to 10 MHz. Although piezoelectric sensors are the most commonly used for AE measurements, we note that other types of sensors exist, such as piezoresistive sensors or laser interferometry based systems.

A relatively novel technique for measurement of vibrations and AE is based on fiber optical distributed sensors. Recent advances of fiber optic technology offer possibilities for real time monitoring of distributed acoustic emissions in civil structures using large sensor arrays (see, e.g., Measures, 2001, and references therein) or for application as hydrophone array (Bucaro et al., 1977; Jarzynski et al., 1981). Various techniques have been implemented for measuring acoustic waves by means of optic fibers that capitalize on mechanical interaction induced by elastic waves and optical alteration of light propagating in the affected fiber optical element (Zhang et al., 2004). Excited acoustic waves produce a periodic modulation of the refractive index and light propagation in the fiber is diffracted backward, giving rise to a frequency-shifted component by a phenomenon similar to the Doppler shift (Inaudi and Glisic, 2005). Bragg grated fibers (see e.g., the review of Othonos, 1997; Kageyama et al., 2005; Li et al., 2009) contain photosensitive notches at a specific spacing. If the length between notches varies due to extension or compression of the fibers, light reflection is modified. Strain measurements obtained in such way from fiber-optic cables embedded in concrete parts has been used to locate changes in the integrity of large civil structures (Maaskant et al., 1997). Fast interrogation allows to obtain strain measurement sequences resolving the interaction of elastic waves with optic fibers at comparable frequencies as conventional AE sensors. A direct comparison between fiber-optic based AE measurements and piezoelectric sensors was performed by Chen and Ansari (2000), showing that both methods are able to capture AE signals with a similar sensitivity.

For analysis of a transient acoustic emission signals it is necessary to introduce a threshold separating acoustic events (i.e. those parts of the signal that are associated with failure) from unavoidable noise (Fig. 2, bottom panel). An AE event starts when the signal amplitude exceeds the prescribed threshold (that may be fixed or self adjusting to the noise level). If during an event the signal remains below the threshold for longer than a pre-defined duration (often termed duration–discrimination time or rearm time) the event terminates. In that way AE events may consist of many signal oscillation cycles taking account of the fact that mechanical generation processes typically generate entire wave packages. Most commercial AE acquisition systems offer triggered monitoring operating after this principle. Signal threshold and the discrimination time normally have to be chosen by the user and may vary between different applications.

After determination of events further analysis can give more precise information about the captured AE signal: the event amplitude is the maximum amplitude reached during an AE event; the event duration is the time difference between the first and the last threshold crossing; the rise time is the time difference from the first threshold crossing to the event amplitude. An integration of the square of the signal deviation from its average gives a measure of the wave energy captured by the sensor. Such characteristic numbers are used for operational AE testing since they typically deliver enough information necessary to characterize AE events, without having to treat the entire signal. For a comprehensive review of parametric analysis of AE events see Grosse and Ohtsu (2008).

Capturing the complete transient waveform of individual AE events allows their further analysis by possibly transforming signals into frequency domain. We note however, that because of above mentioned frequency dependent sensitivity of many piezoelectric AE sensors, the frequency content of a signal is often subjected to natural, inevitable band-pass filtering. Despite limitations due to the sensor intrinsic bias, and sensor-signal interaction (reflection of elastic waves, mode conversion, etc.), frequency content of a signal in some cases allows inference of corresponding sources of elastic waves.

3. AE sources and signal propagation

Various types of rapid mechanical deformation in geologic or artificial granular materials have the potential to generate acoustic waves, eventually involving particle interaction such as grain-to-grain impacts, bursts of elastic energy during contact point release, creation of interfacial energy during fracturing, or solid and liquid bond rupture. Following the triggering of an AE event, the elastic waves propagate away from the source location, born by the solid particle network or liquid within the porous material. Elastic wave-medium interactions and the properties of the granular medium may alter the wave (frequencies and amplitudes) and shape its propagation path. Acoustic wave alteration may be attributed to different types of phenomena, such as dispersion (wave velocity depends on frequency, e.g., Liu and Nagel (1993)), attenuation due to viscous contact deformation (e.g., Zhao et al., 2008), attenuation due to frictional dissipation (Brunet et al., 2008), reflection at interfaces (Jia, 2004; Tournat and Gusev, 2009) or other nonlinear effects (e.g., Tournat et al., 2003, 2004). After alteration of the AE wave from propagation, it may undergo changes during detection by the transducer and conversion to analog or digital signal (as mentioned in the previous section). Otherwise the ultimate sink of the released energy is heat production (Gilardi and Sharf, 2002).

3.1. Particle interactions in granular geologic media

Mechanical interaction of particles within granular material play a prominent role for elastic wave generation and propagation. We therefore start with a brief review of mechanical properties of grain contacts. The forces and deformations that occur at a contact point of two ideal spheres were first studied by Hertz (1882). Invoking several simplifying assumptions (most importantly smoothness of contact surfaces and absence of friction), Hertz (1882) derived the contact force F_n as a function of the normal displacement u_n at the contact point,

$$F_n = \frac{2}{3}\frac{E}{1-\nu^2}R^{\star 1/2}u_n^{3/2}, \tag{1}$$

where $R^\star$ is the effective radius ($1/R^\star = (1/R_1 + 1/R_2)$ with R_1 and R_2 the radii of the contacting particles), E is the Young's modulus, and ν is the Poisson's ratio. Hertz' (1882) expression suggests a similitude of curved contacts with a non-linear spring: the stiffness of a two-sphere contact, i.e., the ratio between the contact deformation u and the contact force F, is a nonlinear function of the deformation $F \sim u_n^{3/2}$ (as can be seen from Eq. (1)). This non-linearity has a number of implications for the mechanical and acoustical behavior of granular materials, some of which will be discussed next. The theory of Hertz (1882) was subsequently extended by Mindlin and Deresiewicz (1953) who considered micro slip of the contact and the dependence of contact forces on loading history in the presence of friction.

Hertz' (1882) contact model and its extensions (see e.g., Johnson, 1985, and references therein) determine primarily the normal and tangential elastic deformations at a particle contact. The dynamical behavior of granular materials are, however, strongly affected by non-elastic, dissipative forms of granular interactions (e.g., Hardy et al., 1971; Hutchings, 1979; Kogut and Komvopoulos, 2004). Incomplete restitution of elastic energy during collisions and friction are two forms of energy dissipation that decrease kinetic energy of particles in motion. This phenomena, known as "granular cooling", exemplifies the large dissipative capacity of granular materials (Wolf et al., 1998). In analogy with the thermodynamical description of molecular gases, the random kinetic motion of particles in granular material is termed "granular temperature" (Goldhirsch, 2008). As a measure of available kinetic energy within an entrained assembly of particles granular temperature stands in a close relationship with collision-generated AE. In fact there exist several attempts to quantify granular temperature within experimental systems using event rate or energy of acoustic emissions (e.g., Cody et al., 1996; Jiang et al., 2007). Granular temperature, together with density and stress, is one of the properties that determine jamming or unjamming of particles, i.e. the spontaneous onset or loss of rigidity, within granular matter (Levine, 2001). The concepts above suggest that yielding of granular materials under shear stress may be viewed as continuous fluctuations around a jamming–unjamming limit associated with localized increase in granular temperature. Numerical simulations of granular materials provide clear evidence of the link between bursts of kinetic energy and shear deformation (e.g., Tordesillas, 2007; Welker and McNamara, 2011). Potential usefulness of such phenomena for AE-based detection of shear failure will be discussed in the next section.

3.2. Sources of acoustic emissions in granular geologic media

There is a wide array of failure mechanisms that may generate acoustic emissions in geologic granular media. Fig. 3 presents the most prominent ones, such as rupture of plant roots, breakage of cohesive soils aggregates, crackling of soil particle cementation, friction between particles, release of contact force between particles or the rupture of capillary bridges. In the following we review mechanisms of AE generation in geologic granular material and introduce four classes of source mechanisms that may vary in their relevance for different scenarios and representations of granular materials. Also we note that elastic waves in complex natural geologic materials are presumably not generated exclusively by one source mechanism but rather by a combination of processes. Simple theoretical considerations will be presented for several types of source mechanisms that may guide estimates of amplitudes, frequencies and other features of generated acoustic emissions.

3.2.1. Acoustic emissions induced by grain contact networks rearrangement

It has been demonstrated (Job et al., 2005, 2008) that the impact of a single grain on a particle chain, as well as the collision of a striker with a granular bed (Rioual et al., 2000) or a rigid surface (e.g., by Henrique et al., 1997; Carson et al., 2008) often generate elastic waves. Rapid and energy-dissipative rearrangements of microstructure within granular materials, such as the instantaneous formation of contacts, may result in significant internal particle collisions and therefore play a role in AE generation. Studies have shown that even minor deformation of granular material may be associated with a large number of such rearrangement events (e.g. Thornton, 2000; Li and Aydin, 2010; Welker and McNamara, 2011). In addition to grain collisions, we may also consider the abrupt removal of existing contacts and associated rapid release of elastic energy as a potential source of AE. For most cases of slow progressive failure of geologic granular materials this presumably outweighs rapid grain collisions (Longhi et al., 2002). For understanding grain force release and associated AE generation it is prerequisite to investigate the distribution of contact forces within a granular assembly.

Granular Earth materials, such as soil or sand, are typically polydisperse and disordered. Considering inherent hindrances to attaining most energetically favorable internal configuration when being

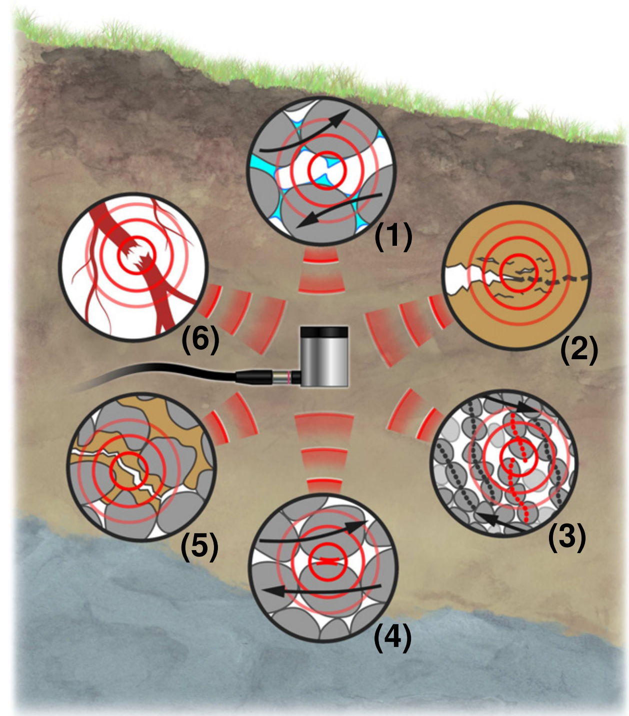

Fig. 3. Different representations of source mechanisms proposed for the generation of acoustic emissions in granular geologic materials: (1) liquid bridge rupture, (2) crack development, (3) release of force chains, (4) grain friction, (5) grain cementation fracture, and (6) rupture of soil fibers.

externally loaded, a typical occurrence is the inhomogeneous distribution of loads amongst contacting particles. Within the force network (i.e., all particles and particle contacts that participate in internal stress redistribution) one may find that a small fraction of grains are bearing disproportionally high loads. Load bearing particles are usually aligned roughly in the direction of principal stresses and often called force chains. Force chains can be observed in experiments (Løvoll et al., 1999; Behringer et al., 2005; Rechenmacher et al., 2010) as well as in numerical simulations (Radjai et al., 1996). Liu et al. (1995) proposed the following distribution to account for inhomogeneities of contact forces in granular material F:

$$P(F)\sim\begin{cases} F^{\alpha} & \text{if } F\leq\hat{F}; \\ e^{-\beta F} & \text{if } F>\hat{F}. \end{cases} \tag{2}$$

Based on theoretical considerations Liu et al. (1995) suggested a power law distribution of forces for the weak contact network (all contacts that bear less than the average force $\hat{F}$) with characteristic coefficient α and a exponential distribution for forces of the strong contact network (contacts that bear more than the average force), with exponential coefficient β. This relations were confirmed experimentally (e.g., Løvoll et al., 1999) and by numerical simulation (Radjai et al., 1996). In their Couette cell experiments Behringer et al. (2005) were able to show continuous breakage and reformation of such force chains in granular material under shear deformation. These findings support the notion that acoustic emissions from grain contact rearrangement may be strongly enhanced by heterogeneous force distribution in disordered granular materials, especially through high force concentrations, associated with so-called force chains. The failure of such force chains results in abrupt release of relatively large amounts of elastic energy which by itself may generate elastic waves. The force distribution within the contact network constituted by such force chains, as given in Eq. (2), may serve as a starting point for estimation of the amount of energy available for elastic wave generation.

The link between force chain associated rearrangements and acoustic emissions was underlined by Hidalgo et al. (2002), who measured AE events from an uniaxially loaded assembly of glass beads. Hidalgo et al. (2002) have introduced a statistical model based on the assumption that newly formed force chains appear with increasing load before force chain formation ceases at a saturation load. Increasing loading at the same time induces failure of individual chains. Subsequent force redistribution is modeled using a variation of the so called fiber bundle model (for a description of the fiber bundle model see e.g., Raischel et al., 2006b, or Section 6 of this paper). These authors have found a good match between magnitude–frequency distribution of observed acoustic events and statistical characteristics of modeled force restructuring events, giving further indication for the production of AE events by such force network rearrangement.

The onset of shear deformation in most granular materials is associated with the formation of a shear zone in the process of strain weakening (see e.g., Read and Hegemier, 1984, and references therein). Local deformation induces weakening of the affected zones which leads to further attraction of strain and facilitates the localization of a slip plane. Localization of strain along a shear plane or shear bands in granular geologic material has been treated by a number of authors (e.g., Mühlhaus and Vardoulakis, 1987; Bardet and Proubet, 1991; Desrues and Viggiani, 2004; Gardiner and Tordesillas, 2004; Ord et al., 2007). Shear band formation is known to be preceded by characteristic patterns of grain rearrangements, namely the promotion of a strong contact network (force chains) bearing disproportionally high loads (Radjai et al., 1998; Majmudar and Behringer, 2005), appearance of rolling (e.g., Mueth et al., 2000; Alonso Marroquin et al., 2006; Estrada et al., 2008) and sliding (e.g., Thornton, 2000) particle contacts. Evidence also suggests a preferential orientation of the strong network along the major principal stress direction (e.g., Gardiner and Tordesillas, 2005; Estrada et al., 2008). Once a shear zone has been formed, episodic fluctuations of the average number of grain contacts (coordination number) and the local density within the shear zone would be accompanied by sequences of unjamming (shear flow within the mobilized layers of the material) and jamming (hampered shear) (e.g., Cain et al., 2001; Aharonov and Sparks, 2004; Alonso Marroquin et al., 2006). Fluctuations in average contacts per particle also illustrate the continuous destruction and reformation of contact points – an indication that shear zones once formed within a granular material have the potential for emission of elastic waves due to intermittent destruction and formation of contact points.

As pointed out in the previous section there are close relations between the granular temperature (i.e. the random kinetic energy of particles) and the jamming–unjamming transition respectively the onset of shear inside a granular assembly. Tordesillas (2007) observed a localized increase of the fluctuating kinetic energy during shear band formation and severe bursts of this quantity during subsequent stick–slip motion in their 2-D simulations of biaxial tests. Comparable features of spontaneous grain network reformations were observed in a numerical simulation of a gradually tilted granular bed by Staron et al. (2006), reporting an increase in the total kinetic energy of the sloping bed as precursors of large avalanches. In addition they observed a strong increase in contact reformations prior to large failure events. Welker and McNamara (2011) conducted detailed numerical analysis of failure precursors during biaxial tests on granular media and reported small rearrangement events prior to failure. The signature of such rearrangements is again clearly visible as localized bursts of particle kinetic energy within the system. Additionally such precursor events involve sudden changes in the number of sliding contacts. In their work Welker and McNamara (2011) have postulated that measurement of such precursory events and bursts of kinetic energy should be possible by means of acoustic emission method.

3.2.2. Acoustic emissions generated by motion of liquid–gas interfaces

Chotard et al. (2006) demonstrated that water evaporation from porous ceramic induced numerous AE events. Similar measurements, taken from tree trunks during water stress that induced cavitation within tree xylem vessels, produces rich acoustic emissions that were used to characterize the level of embolism in the xylem (Tyree and Sperry, 1989; Zweifel and Zeugin, 2008). Hung et al. (2009) measured acoustic emissions induced by water flow through gravel to quantify seepage in dams. DiCarlo et al. (2003) observed considerable elastic wave generation during imbibition and drainage of sand columns expressed as hydroacoustic signals (propagating primarily through the liquid phase).

These experimental studies demonstrate that rapid motions of gas–liquid interfaces in bulk liquid (i.e., bubbles) or in porous media (fluid displacement fronts) may produce significant and measurable AE. They provide indication that measured AE signals are related to abrupt fluid motion when invading or escaping individual pores (Haines jumps). Chotard et al. (2006) attributed elastic wave generation to snapping air water interfaces associated with gas phase invasion. DiCarlo et al. (2003) propose that either rapid acceleration or deceleration of liquid–gas interfaces or subsequent oscillations of the liquid body may be responsible for triggering acoustic waves. Many fluid displacement processes in granular porous media that appear macroscopically continuous may result from numerous microscopic discontinuous rapid interfacial jumps. Given the abrupt nature of pore filling and emptying events induced by macroscopic wetting front displacement during shearing of wet granular media, it seems reasonable to include such jumps into the family of potential acoustic emission sources. In this review we shall concentrate primarily on one process involving rapid motion and reconfiguration of liquid interfaces, that is probably most closely related to shear deformation of wet granular material: namely the rupture of capillary bridges and liquid clusters between particles as depicted in images taken with a high-speed camera in Fig. 4. Characterization of the primary forces at play in this phenomenon is key to understanding AE generation, hence, these will be reviewed in the following.

The surface tension and the internal fluid pressure contribute to a tensile stress that a liquid bridge exerts on the attached particles (given the liquid is the wetting phase). If such a bridge is stretched due to mechanical deformation it ultimately breaks at some critical elongation distance (see Fig. 5) and the elastic interfacial energy stored in the deformed bridge is rapidly released as the newly formed bodies of water seek a configuration of minimum interfacial

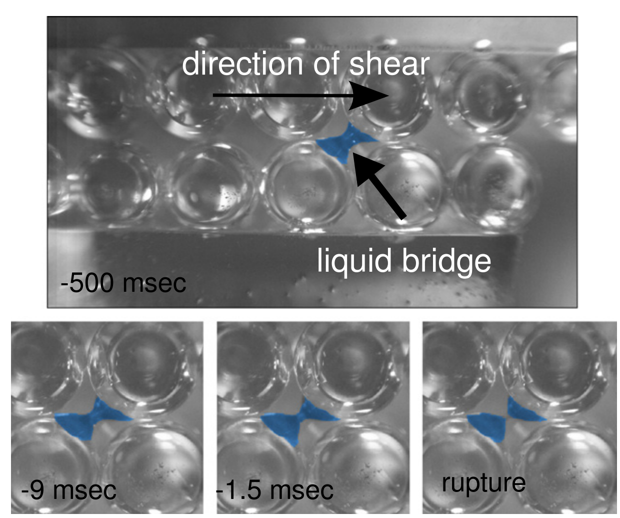

Fig. 4. Rupture of a liquid bridge between two layers of glass spheres (diameter = 4 mm) sheared towards each others. The series shows that the liquid bridge remains stable until a few milliseconds before final rupture, when a slender liquid thread develops that ultimately leads to failure.

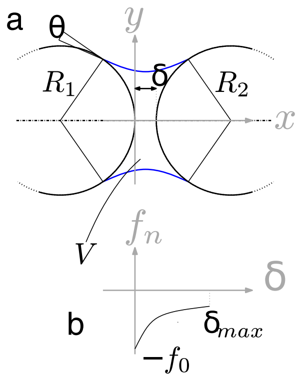

Fig. 5. (a) Liquid bridge rupture during shear deformation in wet granular material. (b) Decay of tensile (negative) contact force with distance between two spheres. (after: Richefeu et al., 2006).

energy. The released energy (deduced from the bridge geometry) provides an upper bound for the energy of triggered acoustic emissions.

Invoking Fisher's assumption (Fisher, 1926) for approximating the shape of a liquid bond between two spheres as toroids and the well known Young-Laplace equation (relating the capillary pressure with the inverse radii of curvature and the surface tension) yield an analytical description of the static bridge force. This functional expression includes interface contact angle θ, the liquid surface tension γ, the harmonic mean R^* of the grain diameters R_1, R_2 $(1/R^* = (1/R_1 + 1/R_2))$, the normalized liquid volume $V^* = V/R^3$ and the separation distance δ (see Fig. 5). Generally speaking (e.g., Pierrat and Caram, 1997), the capillary force decreases with increasing grain separation distance δ. Integration of the bridge force over the separation path determines the rupture energy W_{rup} released during liquid bond rupture (Simons and Fairbrother, 2000). Pitois et al. (2001) refer to the following semi-empirical expression for the scaled rupture energy:

$$\frac{W_{rup}}{\gamma R^{*2}} \approxeq \frac{2\sqrt{V^*}}{0.45 - 0.08\theta + 0.3\theta^2} \tag{3}$$

The rupture energy defining the maximum available energy for AE generation is relatively small: Rupture of water ($\gamma = 0.072$ N/m) bridges between mm-sized ($R = 0.001$ m) glass beads ($\theta \approx 0$) at 11.6 % water content (corresponds to $V^* = 0.043$, see Mason and Clark (1968, Table 1)) according to Eq. (3) releases energies in the 0.1 μJ-range (10^{-7} J).

Analysis of dynamical deformation of capillary bridges performed by Chen and Tsamopoulos (1993), Mollot et al. (1993), Zhang et al. (1996) have shown by numerical simulations (as confirmed in experiments) that the rupture process involves the formation of a thin liquid thread between the two separating liquid bodies that elongates and finally breaks. The time of formation and breakage of this slender fluid thread is only weakly dependent on the experimental conditions. Zhang et al. (1996) provide a typical timescale in the range of 1–20 ms for the rupture of a liquid bridge.

In granular or porous media, small amounts of liquid may form complex bond networks between grains and form clusters of particles held together by capillary forces (e.g. Mitarai and Nori, 2006; Grof et al., 2008; Scheel et al., 2008). Deformation of wet granular material usually perturbs the bridge network and eventually leads to rupture of cohesive liquid bonds (Fournier et al., 2005; Mitarai and Nori, 2006). Richefeu et al. (2006) performed numerical simulations of direct shear tests with wet granular material and observe a decrease of liquid bonds between grains within the shear zone during deformation particularly when the material undergoes dilation, i.e. volumetric expansion at the onset of shear. According to the results of Richefeu et al. (2006) the coordination number for tensile bonds decreases by almost one within the first four grain diameters of shear deformation. In other words each grain within the shear zone experiences in average one liquid bond rupture at the onset of shear. Liquid bridges between single grains in general prevail at low degrees of saturation where most of the pore space is occupied by air. With increasing water content large connected clusters of liquid form as coalescence of many bridges, which ultimately inhibit occurrence of liquid breakage. This regime is often termed "funicular" (Herminghaus, 2005; Mitarai and Nori, 2006) and favors liquid displacement by means of flow above violent breakage events. Correspondingly it would be reasonable to expect less AE activity due to liquid–gas interface displacement at higher degrees of saturation. It is worth to note that Goren et al. (2010, 2011) demonstrated the presence of considerable liquid pressure fluctuations due to mechanical coupling of pore fluid and grains during shear deformation. Abrupt pore liquid pressure changes are generated from shear induced variations of porosity (as described e.g. by Aharonov and Sparks (2002)) within the slip plane. Although not to be counted as liquid–gas interface motion in the strict sense, fluctuations of pore liquid pressure may present a further mechanism to generate acoustic or hydroacoustic (born by the pore liquid) emissions.

3.2.3. Acoustic emissions generated by grain friction

Frictional processes are often associated with vibration, elastic waves or audible sound (Akay, 2002) in engineered systems (e.g., Ibrahim, 1994a,b; Patitsas, 2010) and in geologic materials (e.g., Sammonds and Ohnaka, 1998; Yabe, 2002; Yabe et al., 2003; Yabe, 2008). Friction induced elastic waves or vibrations may be generated from the following processes: abrasion and deformation of asperities at the contact surface (Yabe, 2008; McLaskey and Glaser, 2011), wear and grinding of debris between the surfaces (e.g., Jiaa and Dornfeld, 1990), abrupt localized acceleration due to unlocking of the contact asperities and rapid reduction of frictional force (e.g., Radjai et al., 1995). (Yabe et al., 2003) have shown generation of elastic waves with frequency contents in the kHz range from frictional sliding of two granite surfaces pressed against each others with a pressure of 10 MPa. Measurements of the surface roughness before and after those tests revealed considerable wear of asperities and a smoothening of the rock surfaces as a consequence of sliding experiments. Estimations of the elastic wave source radius suggest that the coherent breakage of asperities at a certain location is responsible for single acoustic emission events. Slider experiments at relatively lower confining pressures (~100 kPa) were conducted by McLaskey and Glaser (2011) or Zigone et al. (2011) and gave indication that elastic waves are

Table 1
Literature review of wave frequencies from different AE source mechanisms.

AE mechanism	char. time	Literature source	test procedure	char. freq.
grain collision	$10^{-6}-10^{-5}$ s	Jiang et al. (2007)	AE measurements of wall grain collisions in a fluidized granular flow	20–80 kHz
		Cody et al. (1996)	Accelerometer measurements of glass bead-container wall collisions in a fluidized granular bed	10–20 kHz
fluid interface displacement	$10^{-3}-10^{-2}$ s	Hung et al. (2009)	AE from water flow in natural soils	0.8–10 kHz
frictional sliding of grains		Gardel et al. (2009)	sliding of grains against a silo wall during discharge	<10 kHz
grain/rock fracture		Read et al. (1995)	3-axial testing of porous rock	100–600 kHz

generated by single asperity failure. Comparison to synthetic waveforms indicate sudden force release events of 1–100 mN in magnitude to trigger acoustic emission events.

Friction is often described by the Amontons-Coulomb law, in which the force opposing relative tangential motion of two contacting bodies is proportional to the normal stress at the contact plane. A constant sliding friction coefficient μ is typically introduced to express the relation between normal and friction forces (see e.g., Bowden and Tabor, 2001). Experimental evidence suggest limitations to the Amontons-Coulomb relation as the friction coefficient μ appears to depend on a number of different factors, such as relative velocity of the contact pair, surface wear or temperature (Ibrahim, 1994b; Rice et al., 2001). This may result in considerable fluctuations of the friction force despite constant normal load. The dependence of μ particularly on sliding velocity eventually leads to the formation of different friction regimes such as creep motion, stick–slip sliding (stalled motion interrupted by phases of intermittent slip) or steady sliding (Heslot et al., 1994). Experiments showed that magnitudes of friction force jumps Δf at a constant normal force often possess a power-law probability distribution of the form $P(\Delta F) \sim 1/\Delta F^{\alpha}$, α being a constant factor. Experimental evidence of such power-law features in dry frictional systems was found by Ciliberto and Laroche (1994, 1999), Buldyrev et al. (2006) or Duarte et al. (2009). At the same time statistics of AE monitored friction between surfaces on a large span of length scales resemble a power-law behavior (e.g., Weeks et al., 1978; Liakopoulou Morris et al., 1994; Sammonds and Ohnaka, 1998).

Obtaining a functional form of μ (including its dependence on temperature, sliding velocity etc.) for heterogeneous material represents a major challenge (Rice et al., 2001). Conversely, there are several statistical–conceptual models relying on individual representation of asperities and humps of the contacting surfaces or arrested pieces of debris, with simple failure and interaction laws. Characteristic ongoing fluctuations around a critical state (e.g. the verge of sliding and arrested motion) are often referred to as self-organized criticality (Bak et al., 1987, 1988) and can be represented well with such models. Examples are the Robin-Hood model of self-organized criticality (Zaitsev, 1992) that was used by (Buldyrev et al., 2006) to reproduce characteristic force jumps during friction tests (using a pin-on-disk tribometer) or variants of the fiber bundle model (e.g., Raischel et al., 2006b) for the description of creep (Kun et al., 2006). We emphasize that failure of individual structural elements and fluctuations of the friction force, both of which are central features of SOC models, are assumed to be the main mechanisms to generate elastic waves during friction.

It is widely recognized that frictional interaction at particle contacts occurs during deformation of granular material. The importance of grain-to-grain friction was demonstrated in various numerical (Thornton, 2000; Cui and O'Sullivan, 2006) and experimental (Behringer et al., 1999; Pohlman et al., 2006) studies. It has been shown by Tordesillas and Muthuswamy (2009) that microslip events (i.e., frictional slip events of single grain contacts) exert a large influence on the collapse of force chains as they typically affect the weak contacts delivering support for highly loaded grains. Thornton (2000) demonstrated with numerical simulations that more than 10% of all contact points are sliding in a granular packing that undergoes shear deformation. Y. Wang et al. (2009) performed triaxial tests on samples of loose sand and attribute high rates of observed acoustic emissions primarily to the frictional interaction of sand particles.

3.2.4. Acoustic emissions during crack formation

The formation and growth of cracks is a hallmark of brittle failure, which is probably the most common type of material damage monitored by acoustic emissions. An overview of different models of crack formation and fracture progression was given by Vanel et al. (2009). In granular earth materials cracks occur within solid cohesive grain bonds or during abrasive wear or splitting of single particles. Fracturing of grains usually requires high confining loads, that may however be provided even at moderate loading conditions due to inhomogeneous force distributions and stress concentrations at particle contact points. Elastic waves generated during fracturing of brittle solids strongly depend on the crack mode (tensile crack, shear crack or mixed mode crack) and the failure plane orientation, but are also influenced by material elasticity. Sophisticated tools, such as moment tensor analysis, facilitate prediction of amplitudes, frequencies and wave modes emanating from crack opening events in brittle media such as concrete or rock (Stump and Johnson, 1977; Kanamori and Given, 1981; Dahm, 1996; Grosse and Ohtsu, 2008). Moreover, certain statistical features of fracture growth are relatively well understood (see e.g., Toussaint and Pride, 2002a,b,c; Girard et al., 2010) and provide a sound basis for analysis of acoustic emissions due to brittle failure.

Changes in chemical or physical conditions (pH, temperature, water content) in soils may promote precipitation of different solute species from soil water. An example is the development of Al- or Fe-oxide crusts. In arid climates the extensive precipitation of Ca-compounds can lead to grain cementation (Ismail et al., 2002). Fig. 6 shows scanning electron microscope images of such grain cementations. In addition to inorganic grain cementation, biological activity (plants, fungi, microbes) may promote formation and enmeshing of soil particles giving rise to aggregation and secondary structures (Tisdall and Oades, 1982). Growing roots and soil microbes release primarily polysaccharides and polyuronides that have gel like consistency under hydrated conditions, but become stiff and rigid as soil dries (Or et al., 2007). Plant roots play a prominent role for mechanical soil

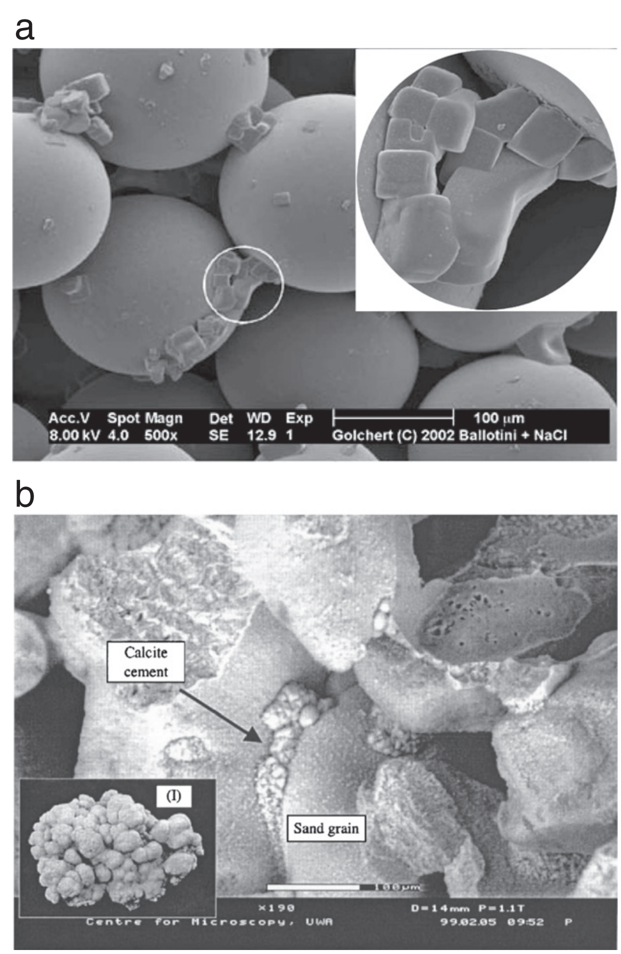

Fig. 6. ESEM micrograph of cemented grains: (a) (from Golchert et al., 2004) shows the formation of sodium chloride precipitates at the contact points of granular material. (b) (from Ismail et al., 2002) illustrates calcite crusts cementing grains.

reinforcement (e.g., Gray and Leiser, 1982). Schwarz et al. (2010) and Cohen et al. (2011) have recently shown the complexity of rupture of root reinforced soils. Breakage or slippage of individual roots respectively the accumulation of such events represent important failure mechanisms preceding hydromechanical collapse of natural soils (e.g., during landslide release). Considering the fact that straining wood or other fibrous plant tissues is often associated with generation of AE (e.g., Grosse and Ohtsu, 2008, chap. 12 and references therein), we may expect strong root associated acoustic activity of mechanically stressed root-reinforced soils.

The generation of AE by the breakage of grain cementing agents was demonstrated by Y. Wang et al. (2009), who observed significant increase of acoustic emissions during triaxial tests of cemented sands. The work of Y. Wang et al. (2009) is probably one of the few studies that reported measurements of elastic waves associated with grain bond failure. Nevertheless, a significant amount of scientific work was undertaken to analyze elastic waves from other natural composite or porous materials such as sandstone, gypsum or snow. Although the behavior of those materials could be markedly different than that of cemented soil, certain insights concerning AE could be gained from these studies. Acoustic emissions in sandstone were measured during loading e.g., by Mlakar et al. (1993) (uniaxial stress tests), Zhang et al. (1990) (hydrostatical compression), Baud et al. (2004), Liakopoulou Morris et al. (1994) (triaxial tests), Mayr et al. (2011), Dresen et al. (2010) (fluid pressure increase) and Schubnel et al. (2007) (combined triaxial and pore pressure loading). Experiments concerning mechanical loading of sandstone have frequently used rates of AE events to distinguish different stages of deformation (matrix crackling, grain crushing) as well as to determine the type of ongoing collapse (localized or diffuse failure). Schubnel et al. (2007) demonstrated that acoustic emissions occur prior to hydromechanically induced rock fracture and allow to follow progressive damage accumulation within the material. Read et al. (1995) studied the dominant acoustic frequencies during loading of Darley Dale sandstone and showed that this parameter changes such that high frequency signals (500 kHz) occur preferably prior to peak stress while the post failure signals are associated with a lower characteristic frequency (100 − 200 kHz), also it was observed that the AE amplitudes significantly increase after exceeding peak stress. Read et al. (1995) associated this frequency shift with the transition from isolated cracks to coalescence and development of system-wide fractures. Zang et al. (1996) distinguished the failure of grain bonds and from frictional sliding of already released grains by analyzing duration and energies of acoustic emissions. High energy events with a duration shorter than 1 ms were generated by fracturing whereas low energy events with longer duration were associated with deformations along existing crack surfaces. Stress jumps during the ductile deformation of gypsum rock samples were monitored by means of acoustic emissions by Brantut et al. (2011), who attributed AE signals inside loaded samples to shear band formation and crack propagation.

Acoustic emissions events were observed in snow samples by McClung (1986) during progressive deformation. Largely enhanced intensity of the AE rate for fast shear delivered indication towards local shear plane formation while imposing slow shear, resulting in little acoustic emissions, pointed towards snow creep. To describe snow avalanche generation from crack propagation at constant loading McClung (1986) makes use of the J-integral introduced by Rice (1968). Palmer and Rice (1973) apply the same principle to the propagation of fractures in overconsolidated clay soils, leading them to the conclusion, that the crack propagation zone, i.e. the portion of the material having a stress field disturbed by the fracture, in such material might attain considerable lengths of 0.5 − 2.5 m.

In addition to cracks forming between grains, AE may also emanate from breakage of grains themselves. Relative to bond rupture, crushing of grains typically requires higher stresses but also releases higher amounts of energy. Grain comminution can be observed in sandstone, e.g. during the formation of compaction bands (Fortin et al., 2006; Stanchits et al., 2009) but also in loose sand. Karner et al. (2003) found that for isotropic loading of loose quartz sand, so in the absence of any grain bonding agents, plastic deformation and significant grain comminution sets in at roughly 100 MPa. Measurements of acoustic emissions during their experiments showed that the rate of AE events shows a significant increase already at a hydrostatic pressure of 40–60 MPa, when the material displays still material behavior. With increasing magnitude of compressive stresses the contact network becomes more and more rigid and the primary sources of AE are asperity breakage and grain microcrackling. Hydrostatic compression does typically not admit large rearrangements of the contact network the development of pre-fracture microcracks and wear of asperities inside the high force network might be considered as potential sources of such AE. The concentration of contact forces in a small amount of grains within the total force network (force chains, see Section 3.2.1) and the concentration of grain-to-grain forces on a relatively small contact area might cause localized development of fissures and microcracks even at moderate loading. Guimaraes et al. (2007) points out the importance of the coordination number for the probability of grain fracture. At low coordination numbers loads on individual particles are concentrated on just a few contact points, which increases the probability of fracture. Analysis based on Hertz contact theory show that stresses around a contact point are not compressional only, but at the circumference of the contact circle tension stresses occur that can induce fracturing of the material in this region (see Fig. 7). These Hertz fractures are described in greater detail by Frank and Lawn (1967) or Wilshaw (1971). In addition to the AE that are generated from the micro-crack development around a contact region, Hertz fractures can also serve as nucleation points for further fracture propagation. Depending on their initial size relative to the particle Hertz fractures can either lead to splitting of grains or induce detachment of small chips from particle surfaces (see Fig. 7).

3.3. Frequency ranges and energies associated with acoustic emissions

Energies and frequency spectra of AE strongly depend on their generation mechanisms. While AE energies can be bracketed for most AE source mechanisms, calculating signal frequencies at the source is typically very demanding. Elastic wave frequency spectra depend, amongst others, on the time scale of energy release, resonance frequencies of involved structures and material properties. In the following we provide a review of maximum available energies

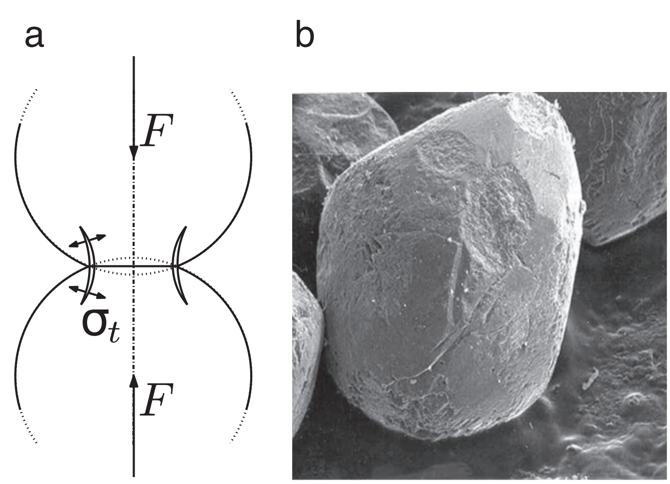

Fig. 7. Grain rupture: (a) Occurrence of localized tensile forces at the fringe of the contact zone between two particles can lead to fracturing of this zone (modified after Zhang et al. (1990)) (b) SEM photograph of a sand grain with chips being split of its surface by Guimaraes et al. (2007).

and source frequency spectra for different classes of failure associated AE in geologic materials. In some cases we will also give time scales τ associated with mechanisms implying a loose connection to the inverse of generated AE frequencies f ($\tau \sim 1/f$).

Using Hertz' contact mechanics the energy required for deformation U is equivalent to the amount of mechanical work and can be obtained from path integration of contact force (given by Eq. (1)). It depends primarily on Poisson's ratio ν, Young's Modulus E and the effective radius $R^{\star}$ of the contacting particles as well as on the maximum contact point deformation u:

$$U = \frac{4}{15}\frac{E}{1-\nu^2}\sqrt{R^{\star}}u^{5/2}. \tag{4}$$

We note that for perfectly elastic conditions this would also be the amount of work stored in a deformed contact. The elastically stored energy can attain large values in the presence of force chains as the affected contacts might undergo strong deformation. The contact deformation energy may be released abruptly during failure of force chains. However it has been shown that the fraction of deformation energy that is dissipated by elastic wave generation is in the range of a few percents only (Hunter, 1957; Hutchings, 1979).

An estimate of the time scale of a particle-wall collision may be deduced from Landau and Lifshitz' energy balance arguments assuming perfectly elastic behavior (Landau and Lifshitz, 1986, see Section 9). Contact time τ of such an idealized collision is expressed as integral function of the initial impact velocity v_0, and the final displacement u_0:

$$\tau = \frac{2}{v_0}\int_0^{u_0}\frac{du}{\sqrt{1-\left(\frac{u}{u_0}\right)^{5/2}}} = \frac{2u_0}{v_0}\int_0^1\frac{d\omega}{\sqrt{1-\omega^{5/2}}}$$
$$= \frac{2u_0}{v_0}\frac{2\sqrt{\pi}\Gamma(2/5)}{5\Gamma(9/10)} \approx \frac{2.94u_0}{v_0} \tag{5}$$

The above approximation predicts that for a 1 mm glass sphere colliding at a velocity of 0.05 m/s into a wall, the impact time would be 13 *μsec*. Following the calculation of Landau and Lifshitz (1986) it can be found that low impact velocities lead to short contact times, while high impact velocities increase the time that particles are in contact. Cody et al. (1996) implied similar assumptions for the estimation of frequencies from grain–wall impacts for fluidized granular material. Using 0.05 − 0.5 mm glass beads colliding with velocities of 0.01 − 1 m/s Cody et al. (1996) estimate an upper bound for the expected frequency spectrum of about 300 kHz.

AE energies for liquid bridge breakage are bound by the rupture energy given in Eq. (3). In their numerical and experimental analysis of liquid bridge dynamics Zhang et al. (1996) found that the breakage time of such a liquid bridge depends only weakly on experimental conditions and is in the range of 1–20 ms. Interestingly Gauglitz and Radke (1990) estimate a similar time scale for the reformation of a liquid bridge in a capillary during snap-off of a gas bubble. Additionally, Lorenceau et al. (2002) observed that the collapse of a gas–liquid interface at the onset of liquid invasion into a glass pipe typically takes about 20 ms. We note that the dynamics of liquid bridges is much slower than the solid particle interaction and may therefore have a significantly distinct frequency spectrum.

Friction of two rough surfaces often display force fluctuations with frequency magnitude distributions of the form $1/\Delta f^{\alpha}$. Buldyrev et al. (2006) showed that the frequency spectrum of friction generated AE is strongly determined by this characteristic distribution. Striving to model AE frequencies for tribometer experiments they found that this $1/\Delta f^{\alpha}$-noise is typically overlaid by the contacting bodies resonance frequencies (for resonance phenomena in tribometer experiments see also the review of Akay, 2002). Correspondingly for granular material resonance frequencies are assumed to be determined mainly by contact stiffnesses and particle masses. A microstructural model for AE energies generated during frictional processes was recently proposed by Fan et al. (2010) and relies mainly on friction and wear of surface asperities.

From experiments with sandstone samples it is known that fracture of bonds is associated with high frequency acoustic emissions. Corresponding measurements were performed by Zhang et al. (1990); Read et al. (1995); Zang et al. (1996, 1998); Baud et al. (2004) and many others. Read et al. (1995) also analyzed the AE spectra generated during deformation of sandstone and found frequencies in the range of 100 kHz.

AE spectra from different source mechanisms are summarized in Table 1. From the Table it can be seen that grain bridge rupture is assumed to generate very low frequency elastic waves, while grain collisions and force chain release events emit vibrations in the range of 10 kHz. Highest frequencies are eventually generated from frictional sliding and fracture.

3.4. Wave propagation in granular media

The properties of a measured AE signal (amplitude, spectral content) and its attenuation are critically dependent on source distance and propagation characteristics. Elastic waves propagation in granular materials are influenced primarily by the grain elastic modulus, structural properties, such as porosity or coordination number, and energy dissipation mechanisms. The loss of AE wave energy is attributed to the growing wave front area as a signal radiates away from the source (geometrical spreading), wave scattering, mode conversion and incomplete transmission at internal boundaries and inhomogeneities of the material (apparent attenuation) and the conversion of wave energy into heat (material losses) (Wang and Santamarina, 2007).

The speed of an elastic wave c within a particular medium is of paramount importance for the understanding and modeling of dynamic behavior of materials. Evaluation of the Hertzian contact theory shows, that wave propagation velocity in dry granular media is proportional to the 1/6-power of the applied confining pressure (Liu and Nagel, 1992, 1993; Liu, 1994; Jia et al., 1999; Gilles and Coste, 2003). The origins of a discrepancy between this theoretical prediction and experimental observations, indicating a 1/4-power dependency is a matter of ongoing debate (for a summary see Somfai et al., 2005). Nevertheless, theory and experiments clearly show that confining stresses in granular materials exert a crucial influence on propagation of acoustic signals. It is worth mentioning that several studies have shown the reverse effect, i.e. an alteration of mechanical conditions by acoustic waves: E.g. Jia et al. (2011) demonstrated how elastic waves may lead to mechanical weakening in a granular packing. Measurements by Domenico (1977) show that the compressional wave propagation velocity in glass beads ranges from 813 m/s to 1571 m/s for confining pressures of 270–3400 kPa. In unconfined sand the propagation velocity can be as low as 280 m/s (Liu and Nagel, 1993). Somfai et al. (2005) pointed out that despite occurrence of large differences in contact forces due to force chain formation, the stiffness of the contact network, and thus the propagation speed of elastic waves, exhibit a much higher degree of homogeneity. Consequently, elastic waves propagate relatively uniform even through a granular assembly that contains a highly non-homogeneous force network.

Descriptions of acoustic wave propagation through heterogeneous porous or granular media (e.g. Gassmann, 1951; Digby, 1981; Armstrong, 1984; Goddard, 1990) usually make use of the effective medium theory, tacitly assuming that wavelengths (given by the ratio between wave speed c and frequency f) exceed the size of particles. Signals, with wavelengths of the order of less than a few grain sizes experience strong scattering at the interfaces between particles. The seismological term “coda wave” has been introduced into the field of granular acoustics by Jia (2004) to describe this phenomenon (in contrast with coherent wave propagation). A strong apparent attenuation of coda waves may lead to highly reduced propagation distances compared to coherent waves. Jia (2004) found a strong susceptibility of such short-wavelength acoustic signals to the internal organization of granular material, as even the change of one contact along the travel path of a coda wave may alter the characteristics of the signal. Tournat and Gusev (2009) showed that a high frequency (and correspondingly short wave length) acoustic signal is decomposed into a highly scattered coda part and a low-frequency coherent part by demodulation along its propagation path through a packing of glass beads. This wavelength-specific decomposition leads to a inherent cut-off of high frequency waves, undergoing strong scattering and therefore quickly attenuating, in heterogeneous media.

Experiments have shown that the presence of water, filling pore spaces between grains, strongly influences wave propagation properties of the medium (Nyborg et al., 1950; Velea et al., 2000; Oelze et al., 2002; Leong et al., 2004; George et al., 2009; Lu and Sabatier, 2009; Griffiths et al., 2010). Capillary bridge forces may provide additional contact stiffness leading to better acoustic propagation, but on the other hand, motion of contact lines and viscous damping may promote attenuation of elastic waves. Significant contributions to the understanding of elastic wave propagation in water-filled granular media were made by researchers focusing on marine sediment acoustics (e.g. Biot, 1956b; Stoll, 1979; Anderson and Hampton, 1980; Buckingham, 1997; Lee et al., 2007). Various models exist to describe elastic wave propagation in porous material under partially (Mavko and Nur, 1979; Lo et al., 2005) and fully saturated conditions (Biot, 1956a,b; Buckingham, 1997). The significance of pore water can be seen in various experimental studies such as by Brunet et al. (2008), reporting changes of elastic wave attenuation in confined sand after the addition of even small amounts of water or the study of Velea et al. (2000), showing strong variations of the wave velocity with changing water saturation.

For their tremendous capacity of granular matter to dissipate energy, as it was discussed in chapter 3.1, granular materials are very efficient attenuators of elastic waves. Apart from strong apparent attenuation of short wavelength acoustic signals, resulting in the coda-wave phenomenon, elastic waves undergo significant damping also due to material losses (Hardin, 1965; Savage, 1965), i.e., dissipation through heat production. Jackson and Anderson (1970) point out that the effects of non-elastic material behavior and frictional dissipation at grain boundaries are important sources of material loss in dry porous rocks. In their review on elastic wave attenuation in air-dry and wet sand Wang and Santamarina (2007) state that for small strains ($\gamma \leq 10^{-5} - 10^{-6}$) (strains caused by acoustic waves have a similar order of magnitude; see, e.g. Brunet et al., 2008) frictional dissipation at grain contacts may become irrelevant and thermoelastic losses presumably deliver the largest contribution to attenuation. In their study the authors also underline the importance of liquid in granular materials for elastic wave attenuation. In water saturated materials, such as marine sediments, viscous losses due to liquid displacement and liquid–solid interaction delivers further contributions to attenuation (Biot, 1956a; Johnston et al., 1979; Stoll, 1979). For a recent review of attenuation experiments in marine sediments see Holmes et al. (2007).

Elastic wave attenuation can be quantified by different measures (Bourbie et al., 1987), probably the most commonly used is the dimensionless quality factor Q and the attenuation coefficient α with dimensions dB/m. Both, the quality factor and the attenuation coefficient consider frequency dependence of damping. While Q can be interpreted as the relative energy loss per one wave cycle (Knopoff, 1964), α is defined as logarithm of the ratio of two amplitudes measured at different distances from the source. Conversion between those two measures of attenuation can be performed, using the wave velocity c and the frequency f, as follows (Bourbie et al., 1987):

$$Q^{-1} = \frac{c}{\pi f}\alpha \tag{6}$$

In unconsolidated loose granular materials attenuation can be as high as 25 dB/cm (Nyborg et al., 1950), which means that elastic waves are attenuated within a few centimeters of propagation in an extreme case. Table 2 gives an overview of various experimental studies concerning elastic wave attenuation within geologic granular materials and underlines the strong variability of this property on influencing factors. There is a general trend that attenuation decreases with decreasing frequency (Lee et al., 2007), increasing confining stresses (Hardin, 1965) and decreasing fluid saturation (Wang and Santamarina, 2007; Griffiths et al., 2010).

4. Statistics of acoustic emissions in granular geologic materials

Given the large number of grain interactions and associated AE generated during these microscale failures we may use statistical characterization of acoustic emissions for non-invasive assessment of the mechanical state (and its evolution) of the stressed sample. Certain statistical signatures of precursor may provide information of reaching a global, macroscopic critical state.

Experiments on rocks and other brittle materials such as concrete, wood, fiberglass, or paper, have shown that acoustic emissions generated during progressive failure display power–law frequency–amplitude distributions (e.g. Mogi, 1962; Scholz, 1968; Hirata, 1987; Lockner, 1993; Anifrani et al., 1995; Garcimartin et al., 1997; Johansen and Sornette, 2000; Salminen et al., 2002) of the form

$$\log N(>A) = a - b\ \log A, \tag{7}$$

where N is the cumulative number of events greater than amplitude A, and a and b are constants. The exponent b varies usually between 1 and 2 and may depend on rock type and degree of heterogeneity (Mogi, 1962), shear stress and confining pressure (Scholz, 1968; Amitrano, 2003), or temperature in fractures produced by thermal stresses (Warren and Latham, 1970). Power–law scalings like Eq. (7) have also been found for waiting time and energy distributions (e.g. Rosti et al., 2010) with b values in the range of 1.2–2 for energy and 1–1.3 for

Table 2
Literature review of elastic wave attenuation in different earth materials under dry and wet conditions.

Literature source	material	wat. cont.	attenuation
Nyborg et al. (1950)	sand	dry	1–7 dB/cm at 10 kHz and 5–13 dB/cm at 26 kHz
	silt loam soil	air dry	1–22 dB/cm at 10 kHz and 5–26 dB/cm at 26 kHz
Koerner et al. (1981a)	sand	dry	0.09 dB/cm at 0.5 kHz and 10.0 dB/cm at 16 kHz
	clayey silt	variable	1.9 dB/cm at dry and 1.0 dB/cm at saturation
Oelze et al. (2002)	various soils	variable	0.1 dB/cm kHz at dry and 1.0 dB/cm kHz at saturation
George et al. (2009)	silt	variable	0.2 Q^{-1} at saturated and 0.02 Q^{-1} at unsaturated conditions (at 20 kHz excitation)[1]
	loamy sand	variable	0.4 Q^{-1} at saturated and 0.01 Q^{-1} at unsaturated conditions (at 20 kHz excitation)[2]
Leong et al. (2004)	mudstone	dry	203–216 dB/m
	residual soil		

[1] corresponds to ≈ 0.12 dB/cm at saturated and 0.03 dB/cm at unsaturated conditions.
[2] corresponds to ≈ 0.26 dB/cm at saturated and 0.001 dB/cm at unsaturated conditions.

waiting times. The scaling in Eq. (7) is identical to the Gutenberg-Richter relation for earthquakes (Gutenberg and Richter, 1954) with b taking on values around 1. These power–law behaviors are indications of scale-free dynamics and are typical of large complex systems with many degrees of freedoms often interpreted in the context of criticality and phase transitions (e.g. Sethna et al., 2001).

Power–law distributions of AE may fluctuate with time, or equivalently with progressive failure or deformation. To better understand earthquake mechanics, pioneering laboratory studies on rocks have measured variations in the b-value of acoustic emissions associated with slip events between rock surfaces (e.g. Weeks et al., 1978) and with brittle rock fracturing (e.g. Lockner, 1993; Grgic and Amitrano, 2009). In general, the value of b decreases with stress or deformation as the system approaches global failure. This indicates a greater proportion of large failure events. Lockner (1993) associated changes in the b-value to various stages of crack nucleation and growth. Lavrov and Shkuratnik (2005) attributed the decrease of b with increasing stress to the coalescence and fracture of larger cracks, indicators of progression towards a macroscopic scale and thus towards global failure. Main et al. (1989) explained the decrease in the b value observed in earthquakes (e.g. von Seggern, 1980; Jin and Aki, 1986) using a fracture mechanics model for increasing stress intensity factor at tensile crack tips with progressive failure. Similar observations of changes in the power–law exponent have been made for concrete (e.g. Carpinteri et al., 2009), wood and fiberglass (e.g. Guarino et al., 2002), and kevlar and fiber-matrix composite vessels (e.g. Anifrani et al., 1995; Johansen and Sornette, 2000) when approaching global failure. These experiments prove that under controlled laboratory conditions, detectable b-value changes linked to AE activity can be used as an indicator of precursor events prior to global failure. In field studies in rock mines (e.g. Kohler et al., 2009; Becker et al., 2010), recordings of AE have shown spatial and temporal variations in b values associated with microcrack formations, differences in rock type, and thermal unloading. Other than for earthquakes and rock mines, observations of changes in the power–law exponent in natural systems are rare: Shiotani and Ohtsu (1999) recorded fluctuations in the power–law exponent during slope failure but failed to find a consistent trend; Amitrano et al. (2005) observed a marked decrease in the power–law exponent of the distributions of signal energy recorded by geophones a few hours before the collapse of a rock cliff.

Statistics of acoustic emissions have also been used to infer properties of granular materials. For example, Chodyn and Zuberek (1992) measured AE frequency-size distributions during cyclic triaxial compression experiments with sand as a function of differential stress. They noted wider distributions with higher amplitudes at higher differential stress which they attributed to failure of larger normal and frictional contact forces between grains. Hidalgo et al. (2002) measured acoustic emission activity during uniaxial compression of glass beads and observed power–law frequency–amplitude statistics which they associated with failures of force chains. Distributions of normal and shear forces in force chains, however, are exponential above the mean (e.g., Liu et al., 1995; Radjai et al., 1996; Mueth et al., 1998; Løvoll et al., 1999; Blair et al., 2001). Under the assumption that the strain energy U in a force chain scales with the square of the force and all that energy is released through a stress wave associated with an acoustic emission, one should find an AE energy distribution that scales with $e^{-\sqrt{U}}/\sqrt{U}$. Observations, however, indicate that AE amplitude is power–law distributed. This mismatch between force and AE statistics may be due to the increasing number of force chains during loading and their gradual stiffening during restructurings. An alternative explanation is that some energy is dissipated, either through attenuation of the stress wave or during creation of new contacts. Thus far, no definite evidence links the distribution of forces in force chains to the distribution of generated acoustic emissions. Finding such a link remains a challenge for future experimentalists and theoreticians.

Statistics of AE offers instantaneous and noninvasive insights into the mechanical state of geologic materials (composed of numerous mechanical elements) during deformation. For brittle geomaterials, the link between AE statistics and the failure process is relatively well established, as it is often related to characteristic power–law behavior. This link, however, remains to be developed and exploited for granular materials. Identifying signatures of acoustic emissions in granular materials that vary statistically during loading and progressive failure may be the most effective way of monitoring natural systems such as soils on slopes in an effort to devise advance warning systems for imminent slope failure.

5. Linking AE with models of progressive failure

The discrete nature of acoustic emissions lies in their association with failure of individual elements, such as a grain bond or a force chain. When an element breaks, the load carried by the element must be redistributed to the remaining intact elements. This load redistribution may lead to secondary failures of elements and triggers avalanches of failures before the load is distributed to a sufficient number of intact elements to return to a (marginally) stable state. If a failure cascade involves all load-bearing elements of the structure, global collapse occurs marking the final stage of progressive failure behavior. Progressive material degradation should also cause avalanches of acoustic emissions. Indeed the accumulation of AE events during failure progression episodes was observed by researchers working on the mechanical stability of geomaterial and a number of studies were mentioned in previous sections. Models capable of describing progressive failure hold great value for the interpretation of acoustic emissions towards identification of predictors for global failure.

A conceptual framework holding such a promise is the fiber bundle model (FBM) which idealizes and represents a disordered material as a bundle of parallel, linear elastic fibers (e.g., Daniels, 1945; Smith and Phoenix, 1981; Hemmer and Hansen, 1992; Pride and Toussaint, 2002; Toussaint and Pride, 2005; Alava et al., 2006). In the classical FBM all fibers have the same elasticity while the stress at which they fail is different for all fibers and is assigned randomly according to a characteristic probability distribution function. When a bundle of such fibers is loaded in tension it exhibits progressive failure behavior: following an increase in stress, the currently weakest fiber breaks and its load is redistributed to the remaining fibers possibly triggering larger burst avalanches. Increasing stress will gradually break the fiber bundle. Although each fiber is linear elastic, the bundle behaves as a non-linear material. Also, frequency-size distribution of avalanches exhibits a cumulative distribution that is power–law with an exponent of 5/2 (e.g., Hemmer and Hansen, 1992; Raischel et al., 2006a; Pradhan and Hemmer, 2008). While simple versions of the fiber bundle model can be described analytically, numerical calculations are used to formulate variants of the model that incorporate more complex rules (for a comprehensive description of fiber bundle models see Raischel et al., 2006b; Pradhan et al., 2010). Although the FBM in its original formulation reproduces purely tensile loading it can be easily adapted to account for creep rupture or shear failure of disordered materials (Kun et al., 2006). By specifying a healing condition for broken fibers the model can also mimic residual strength and stick–slip behavior (Halasz and Kun, 2009) as it occurs in geomaterials at high strains. Using a healing-fiber FBM Reiweger et al. (2009) modeled shear failure of weak snow layers accounting also for resintering of broken ice crystals within the shear zone. Failure mechanisms that govern the collapse of geologic granular materials and that may be represented using FBMs are shown in Fig. 8: Progressive plant root failure were described as representation of a FBM recently by Cohen et al. (2011). Force chains typically form in stressed granular material and their ongoing destruction and reformation is a characteristic feature of shear deformation.

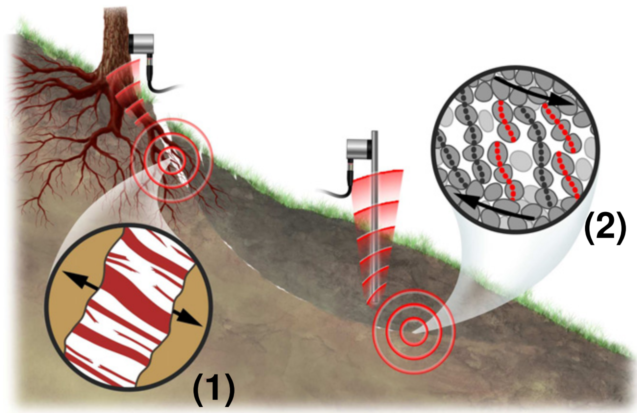

Fig. 8. Fiber bundle model for slope stability monitoring: (1) plant roots and (2) force chains in granular earth material resemble fiber bundles. Similarly their fracture emits acoustic emissions.

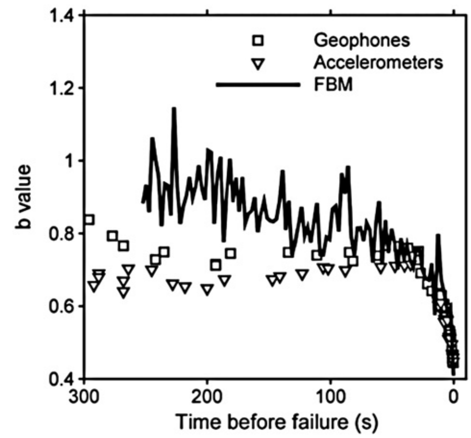

Fig. 9. Correspondence between fiber bundle model statistics and decrease of b-value of microseismic/acoustic measurements prior to a cliff collapse measured by Amitrano et al. (2005). (Figure taken from Cohen et al., 2009).

Simulation of this process using a FBM seems therefore promising and might allow to model force chain associated AE (Hidalgo et al., 2002).

Theoretically a close correspondence between individual fiber failures and associated acoustic emission events are expected. Bursts of fibers during avalanching may release considerable elastic energy generating large acoustic emissions. Some of this energy may be lost in the formation of a new cracked surface and in heat. Bosia et al. (2008) and Pradhan and Hemmer (2008) have estimated energy released during stress loading of a fiber bundle model and predict power–law growth of the cumulative energy and power–law distribution of burst energy. Based on analysis of an overloaded fiber bundle (Pradhan and Hemmer, 2011) predict an energy release minimum preceding failure. The authors propose the acoustic emission method as tool for the detection of such changes in the energy release within a failing material. In modeling fatigue using the so-called dynamic FBM, Turcotte et al. (2003) predict that the cumulative energy as a function of time scaled to the failure time is also power law. These models are in accord with acoustic emission measurements obtained on tensile tests of fibrous materials (e.g. Anifrani et al., 1995; Guarino et al., 1998; Johansen and Sornette, 2000; Carpinteri et al., 2009).

The fiber bundle model predicts that the distribution of event magnitudes evolves during progressive failure (Pradhan et al., 2006) owing to the exponential cutoff of the power–law distribution at high event magnitude. In practice, this change of the shape of the failure distribution has been used to analyze acoustic emission data from failing rocks and fit the change to changes in the power–law exponent b (e.g., Amitrano et al., 2005). Cohen et al. (2009) presented a comparison between the data of Amitrano et al., with the FBM showing the good fit of the model to the data (Fig. 9). Hence, the FBM has the potential to identify precursor events of global failure through identification of changes of the event and energy distribution of fiber bursts. The same method could be applied to acoustic emissions of deforming granular materials although this mechanism has yet to be identified for such materials.

6. Acoustic emissions applications in earth sciences

Table 3 provides an overview of studies reporting the use of AE in granular geologic materials and selected work on other types of granular matter. We mentioned earlier that the first systematic assessment of the AE method for geotechnical applications is attributed to Koerner, who published amongst others a study on AE monitoring of granular (Koerner et al., 1976) and cohesive (Koerner et al., 1977) soils subjected to loading. Koerner recognized the possibilities of AE in field applications and mentioned the importance to find solutions for massive wave attenuation (Koerner et al., 1981a) in soils.

Attempts to circumvent limitations imposed by strong acoustic signal attenuation in soils involve deployment of waveguides (see Fig. 8) especially for field applications. Using metal rods as acoustic wave guides Chichibu et al. (1989) demonstrated that ground displacement in natural slopes generate significant AE. The authors report further that AE signals in some cases were measured days before displacement was visible on the land surface. Similarly Rouse et al. (1991) detected AE (frequency band ranging from 1 kHz to 7 kHz) events using metal waveguides in landslide prone slopes. In their experiments the authors measured a change of the signal characteristics during heavy rainfalls. Although metals have the advantage of being very rigid and therefore easy to deploy, typically there is a strong mismatch of acoustic impedance between them and Earth materials. This can lead to undesirable, strong signal reflections at the interface between the waveguide and the host material. Shiotani and Ohtsu (1999) have addressed issues related to efficient waveguide design for

Table 3
Experiments from the literature involving measurements of acoustic emissions in earth material and other granular media.

Author	experiment
Dixon et al. (2003); Dixon and Spriggs (2007)	Field measurements of an unstable slope using AE
Koerner et al. (1981a)	Measurements of AE during geotechnical testing of soil
Koerner et al. (1981a)	Field measurements of an unstable slope using AE
Chichibu et al. (1989)	Field measurement of AE in an unstable slope, wave-guide application
Rouse et al. (1991)	measurements of microseismic emissions in a landslide prone slope during heavy rainfall
Fernandes et al. (2010)\	AE from oedometer tests with sand
Tanimoto and Nakamura (1981)	AE during triaxial testing of soils specimens
Y. Wang et al. (2009)	AE during triaxial tests with loose and cemented sand
Chodyn and Zuberek (1992)	AE from triaxial tests with sand and from borehole in sand pit
Villet et al. (1981)	AE from cone penetration tests in soils
Huck and Koerner (1981)	AE from hydraulic fractures in soil and rock
Chotard et al. (2006)	AE from water flow during seepage
Mair et al. (2007)	AE form fault gouge between two rock surfaces
Yabe et al. (2003)	AE from frictional sliding of two rock surfaces
Karner et al. (2003)	AE from grain fracture during isotropic loading of sand
Hidalgo et al. (2002)	AE measurements from static glass bead assembly
Gardel et al. (2009)	piezoeletric force measurements during dense granular flow
Jiang et al. (2007)	AE from granular gas random motion

landslide early warning, in which they evaluated the performance of PVC and composite materials as AE waveguides. Dixon et al. (2003), Dixon and Spriggs (2007) propose the use of "active waveguides", i.e. conventional waveguides that are placed in a borehole and backfilled with coarse sand or gravel that generates secondary signals during deformation. Overcoming the issue of acoustic emission attenuation, active waveguides are, however, not designed as a low attenuation link between soil and sensor but to generate acoustic emissions themselves during deformation of the host material.

An attractive natural waveguide could rely on tree roots embedded in soil as a basis for soil failure monitoring (see Fig. 8). Wave attenuation in wood is much lower than in soil. We pointed out in Section 3.2.4 that tree roots constitute a network of natural fibers eventually involved in progressive failure of a natural slope. However the rupture of roots may not be the only source of AE within trees, as also externally produced elastic waves may take advantage of the low attenuation properties within the tree root system leading to detectable root AE. The root system of a tree states a natural network of waveguides that is present in every forested slope. We note however, that tree roots reinforce their surrounding soils and thus may provide a biased picture of locations of landslide initiation (that might develop preferably in areas not reinforced by tree roots).

The presence of ambient noise and electrical noise may lead to erroneous recording of AE events and bias AE based assessment of materials. According to Holt (1976) electronic noise stemming from signal amplifiers or piezo-electric transducers becomes particularly problematic in the testing of quiet samples, that demand a very low signal threshold. The elimination of background noise becomes important in field studies and may lead to the exclusion of a large fraction of recorded events. During their monitoring study at a rockfall site Spillmann et al. (2007) discarded about 99% of the captured microseismic events, mostly for being generated from electronic noise, by applying a semi-automatic exclusion procedure. Raindrop impacts on the measurement equipment may introduce serious errors. (Shiotani, 2006) even for sensors buried at shallow depth. Paparo et al. (2002) pointed out that diurnal air temperature variations may promote significant expansion-contraction cycles of geologic material at the Earth surface, inducing thereby AE activity. During AE monitoring of an unstable coastal cliff Senfaute et al. (2009) observed a strong correlation of tidal sea level fluctuations and observed AE. van Herwijnen and Schweizer (2011a) encountered a large number of different ambient noise sources (vehicle noise, walking noise, etc.) that affected AE monitoring of snow avalanche formation. Koerner et al. (1981a,b) underlines the importance of noise elimination and names frequency filtering, source location filtering, discrimination according to signal shapes and acoustic decoupling of sensors from background noises as most important techniques to perform this task. From their monitoring study of a street embankment Shiotani (2006) conclude, that acoustic shielding of sensors by installing them at larger depths provides a remedy for effects of ambient noise. Despite of a number of studies considering the effect of ambient and electronic noise we are not aware of an work investigating the efficiency of geophysical AE applications as such including false alarm rates or success rates of this monitoring technique.

Recent advances in fiber optic technology and its application to measurement of strains and AEs in geological media offer an exciting array of possibilities for overcoming attenuation and deployment of distributed AE sensing networks (Measures, 2001). Selker et al. (2006) enumerate a list of successful field-scale applications of fiber-optic temperature measurement, which necessitates the very same principles as strain or vibration measurements, and demonstrated usefulness and potentials of the fiber-optic technology for hydrological and geophysical investigations. Successful application of fiber-optic based strain measurements in a geotechnical context were reported by Dai et al. (2008), Iten (2008), B.J. Wang et al. (2009), Zeni (2009), Iten (2011). Although technical specifications vary among techniques and manufacturers, fiber-optic AE measurements may resolve events at meter scale along kilometer long fiber optic cables at very high temporal resolution.

Several studies have attempted to complement standard geotechnical lab tests with different forms of acoustic and vibration monitoring. Examples of AE monitoring during oedometric compression, triaxial tests, cone penetrometer tests, and shear tests can be found in Table 3. A large amount of work has been done for studying different forms of active acoustic emissions in geo-materials: in a review paper on the use of bender elements, i.e. piezoelectric shear wave transducers, Lee and Santamarina (2005) summarize techniques to extract soil mechanical properties from measurement of shear wave that are artificially generated by piezoelectric pulser within the sample material.

7. Conclusions

The implementation of the acoustic emission (AE) method for passive monitoring and characterization of micro scale mechanical failure events in geological material hold a great promise for process understanding and potential early warning systems. The method can be used to observe progressive failure of granular geologic material in lab experiments and to monitor the triggering of landslides or other Earth material movements in field applications, complementary to existing techniques.

We have reviewed elastic waves in granular geologic material released during progressive failure and suggest that their generation is primarily due to grain contact rearrangement (i.e. grain-to-grain collisions and rapid removal of contact points), liquid bridge rupture, frictional sliding and crack formation in grain cementing agents and particles. We found reasonable support for the assumption, that all those mechanisms generate elastic waves within the AE frequency spectrum. Generated acoustic emissions are altered and strongly attenuated while propagation through granular materials. For widely used AE sensing technology based on individual piezoelectric sensors, the usefulness of different acoustic waveguides was demonstrated by a number of studies reviewed in this work. In addition to artificial structures, we propose the assessment of tree roots as natural waveguides, as we are not aware of studies published on this issue. Fiber-optic based sensors present an attractive alternative to point measurements and thus may pave the way to large distributed monitoring networks circumventing issues of signal attenuation limitation AE application over practical field scales of interest.

Amongst statistical methods applicable on AE data records, b-value analysis is maybe most prominent. The b-value is the slope of empirical power–law distributions of occurrence frequencies and changes are known to stand in closed relation with progressive failure of disordered material. We have discussed benefits and potential applications of conceptual statistical models such as the fiber bundle model (FBM) in combination with the AE method to analyze and predict progressive failure evolution in granular geologic materials. Conceptual failure models are able to reproduce pre-failure accumulation of acoustic events and may help to identify changes of AE statistics at imminent failure. Additionally AE measurements bear a great potential to be linked to deterministic discrete element models of granular materials which up to now remain often the only way to investigate grain network changes of micro-mechanical processes within granular materials.

Acknowledgements

This work is part of "Triggering of Rapid Mass Movements" (TRAMM) funded by the Competence Center Environment and Sustainability (CCES) of the ETH domain (Switzerland). The authors would like to thank Dr. Peter Lehmann for valuable comments to improve this manuscript. The manuscript was improved by the comments of three anonymous reviewer to whom the authors want to express their gratefulness.

References

Aharonov, E., Sparks, D., 2002. Shear profiles and localization in simulations of granular materials. Physical Review E 65, 051302.

Aharonov, E., Sparks, D., 2004. Stick-slip motion in simulated granular layers. Journal of Geophysical Research 109, B09306.

Akay, A., 2002. Acoustics of friction. Journal of the Acoustical Society of America 111, 1525–1548.

Alava, M.J., Nukala, P., Zapperi, S., 2006. Statistical models of fracture. Advances in Physics 55, 349–476.

Allan, P., Bellamy, L.J., Nordon, A., Littlejohn, D., 2010. Non-invasive monitoring of the mixing of pharmaceutical powders by broadband acoustic emission. Analyst 135, 518–524.

Alonso Marroquin, F., Vardoulakis, I., Herrmann, H.J., Weatherley, D., Mora, P., 2006. Effect of rolling on dissipation in fault gouges. Physical Review E 74, 031306.

Amitrano, D., 2003. Brittle-ductile transition and associated seismicity: Experimental and numerical studies and relationship with the b value. Journal of Geophysical Research 108, 2044.

Amitrano, D., Grasso, J.R., Senfaute, G., 2005. Seismic precursory patterns before a cliff collapse and critical point phenomena. Geophysical Research Letters 32, L08314.

Anderson, A.L., Hampton, L.D., 1980. Acoustics of gas-bearing sediments. 2. Measurements and models. Journal of the Acoustical Society of America 67, 1890–1903.

Anifrani, J.C., Le Floch, C., Sornette, D., Souillard, B., 1995. Universal log-periodic correction to renormalization group scaling for rupture stress prediction from acoustic emissions. Journal de Physique I 5, 631–638.

Armstrong, B.H., 1984. Models for thermoelastic attenuation of waves in heterogeneous solids. Geophysics 49, 1032–1040.

Bak, P., Tang, C., Wiesenfeld, K., 1987. Self-organized criticality: An explanation of the 1/f noise. Physical Review Letters 59, 381–384.

Bak, P., Tang, C., Wiesenfeld, K., 1988. Self-organized criticality. Physical Review A 38, 364–374.

Bardet, J.P., Proubet, J., 1991. A numerical investigation of the structure of persistent shear bands in granular media. Geotechnique 41, 599–613.

Barre, S., Benzeggagh, M., 1994. On the use of acoustic-emission to investigate damage mechanisms in glass-fiber-reinforced polypropylene. Composites Science and Technology 52, 369–376.

Baud, P., Klein, E., Wong, T.F., 2004. Compaction localization in porous sandstones: Spatial evolution of damage and acoustic emission activity. Journal of Structural Geology 26, 603–624.

Becker, D., Cailleau, B., Dahm, T., Shapiro, S., Kaiser, D., 2010. Stress triggering and stress memory observed from acoustic emission records in a salt mine. Geophysical Journal International 182, 933–948.

Behringer, R.P., Howell, D., Kondic, L., Tennakoon, S., Veje, C., 1999. Predictability and granular materials. Physica D: Nonlinear Phenomena 133, 1–17.

Behringer, R., Clement, E., Geng, J., Hartley, R., Howell, D., Reydellet, G., Utter, B., 2005. Statistical properties of dense granular matter. In: Hoogendoorn, S.P., Luding, S., Bovy, P., Schreckenberg, M., Wolf, D.E. (Eds.), Traffic and Granular Flow 2003. Springer, Berlin, Heidelberg, pp. 431–444.

Biot, M., 1956a. Theory of propagation of elastic waves in a fluid-saturated porous solid 1 - low-frequency range. Journal of the Acoustical Society of America 28, 168–178.

Biot, M., 1956b. Theory of propagation of elastic waves in a fluid-saturated porous solid 2 - higher frequency range. Journal of the Acoustical Society of America 28, 179–191.

Blair, D.L., Mueggenburg, N.W., Marshall, A.H., Jaeger, H.M., Nagel, S.R., 2001. Force distributions in three-dimensional granular assemblies: Effects of packing order and interparticle friction. Physical Review E 63, 041304.

Bosia, F., Pugno, N., Lacidogna, G., Carpinteri, A., 2008. Mesoscopic modeling of acoustic emission through an energetic approach. International Journal of Solids and Structures 45, 5856–5866.

Bourbie, T., Coussy, O., Zinszner, B., 1987. Acoustics of Porous Media, Editions Technip. Paris. 334 pp. (Translation of "Acoustique des milieux poreux").

Bowden, F.P., Tabor, D., 2001. The Friction and Lubrication of Solids. Clarendon Press, Oxford. 374 pp.

Boyd, J.W., Varley, J., 2001. The uses of passive measurement of acoustic emissions from chemical engineering processes. Chemical Engineering Science 56, 1749–1767.

Brantut, N., Schubnel, A., Gueguen, Y., 2011. Damage and rupture dynamics at the brittle-ductile transition: The case of gypsum. Journal of Geophysical Research 116, B01404.

Brunet, T., Jia, X., Mills, P., 2008. Mechanisms for acoustic absorption in dry and weakly wet granular media. Physical Review Letters 101, 138001.

Bucaro, J.A., Dardy, H.D., Carome, E.F., 1977. Fiber-optic hydrophone. Journal of the Acoustical Society of America 62, 1302–1304.

Buckingham, M., 1997. Theory of acoustic attenuation, dispersion, and pulse propagation in unconsolidated granular materials including marine sediments. Journal of the Acoustical Society of America 102, 2579–2596.

Buldyrev, S.V., Ferrante, J., Zypman, F.R., 2006. Dry friction avalanches: Experiment and theory. Physical Review E 74, 066110.

Cadman, J.D., Goodman, R.E., 1967. Landslide noise. Science 158, 1182–1184.

Cain, R.G., Page, N.W., Biggs, S., 2001. Microscopic and macroscopic aspects of stick-slip motion in granular shear. Physical Review E 64, 016413.

Carpinteri, A., Lacidogna, G., Puzzi, S., 2009. From criticality to final collapse: Evolution of the b-value from 1.5 to 1.0. Chaos, Solitons and Fractals 41, 843–853.

Carson, G., Mulholland, A., Nordon, A., Tramontana, M., Gachagan, A., Hayward, G., 2008. Particle sizing using passive ultrasonic measurement of particle-wall impact vibrations. Journal of Sound and Vibration 317, 142–157.

Carson, G., Mulholland, A., Nordon, A., Gachagan, A., Hayward, G., 2009. Theoretical analysis of ultrasonic vibration spectra from multiple particle-plate impacts. IEEE Transactions on Ultrasonics, Ferroelectrics, and Frequency Control 56, 1034–1041.

Chen, Z., Ansari, F., 2000. Fiber optic acoustic emission distributed crack sensor for large structures. Journal of Structural Control 7, 119–129.

Chen, T.Y., Tsamopoulos, J., 1993. Nonlinear dynamics of capillary bridges: theory. Journal of Fluid Mechanics 255, 373–409.

Chichibu, A., Jo, K., Nakamura, M., Goto, T., Kamata, M., 1989. Acoustic emission characteristics of unstable slopes. Journal of Acoustic Emission 8, 107–111.

Chodyn, L., Zuberek, W.M., 1992. Effect of the discrete stress memory in the acoustic emission in soils. Acta Geophysica Polonica 40, 139–158.

Chotard, T., Quet, A., Ersen, A., Smith, A., 2006. Application of the acoustic emission technique to characterise liquid transfer in a porous ceramic during drying. Journal of the European Ceramic Society 26, 1075–1084.

Ciliberto, S., Laroche, C., 1994. Experimental-evidence of self-organized criticality in the stick-slip dynamics of 2 rough elastic surfaces. Journal de Physique I 4, 223–235.

Ciliberto, S., Laroche, C., 1999. Energy dissipation in solid friction. European Physical Journal B 9, 551–558.

Cody, G.D., Goldfarb, D.J., Storch, G.V., Norris, A.N., 1996. Particle granular temperature in gas fluidized beds. Powder Technology 87, 211–232.

Cohen, D., Lehmann, P., Or, D., 2009. Fiber bundle model for multiscale modeling of hydromechanical triggering of shallow landslides. Water Resources Research 45, W10436.

Cohen, D., Schwarz, M., Or, D., 2011. An analytical fiber bundle model for pullout mechanics of root bundles. Journal of Geophysical Research 116, F03010.

Cui, L., O'Sullivan, C., 2006. Exploring the macro- and micro-scale response of an idealised granular material in the direct shear apparatus. Geotechnique 56, 455–468.

Dahm, T., 1996. Relative moment tensor inversion based on ray theory: theory and synthetic tests. Geophysical Journal International 124, 245–257.

Dai, Z.Y., Liu, Y., Zhang, L.X., Ou, Z.H., Zhou, C., Liu, Y.Z., 2008. Landslide monitoring based on high-resolution distributed fiber optic stress sensor. Optical Fiber Sensors Conference, 2008. APOS, pp. 1–4.

Daniels, H.E., 1945. The statistical theory of the strength of bundles of threads. 1. Proceedings of the Royal Society A 183, 405–435.

Desrues, J., Viggiani, G., 2004. Strain localization in sand: An overview of the experimental results obtained in grenoble using stereophotogrammetry. International Journal for Numerical and Analytical Methods in Geomechanics 28, 279–321.

DiCarlo, D.A., Cidoncha, J.I.G., Hickey, C., 2003. Acoustic measurements of pore-scale displacements. Geophysical Research Letters 30, 1901.

Digby, P.J., 1981. The effective elastic moduli of porous granular rocks. Journal of Applied Mechanics 48, 803–808.

Dixon, N., Spriggs, M., 2007. Quantification of slope displacement rates using acoustic emission monitoring. Canadian Geotechnical Journal 44, 966–976.

Dixon, N., Hill, R., Kavanagh, J., 2003. Acoustic emission monitoring of slope instability: Development of an active waveguide system. Proceedings of the ICE: Geotechnical Engineering 156, 83–95.

Domenico, S.N., 1977. Elastic properties of unconsolidated porous sand reservoirs. Geophysics 42, 1339–1368.

Dresen, G., Stanchits, S., Rybacki, E., 2010. Borehole breakout evolution through acoustic emission location analysis. International Journal of Rock Mechanics and Mining Sciences 47, 426–435.

Duarte, M., Vragovic, I., Molina, J.M., Prieto, R., Narciso, J., Louis, E., 2009. 1/f noise in sliding friction under wear conditions: The role of debris. Physical Review Letters 102, 045501.

Estrada, N., Taboada, A., Radja, F., 2008. Shear strength and force transmission in granular media with rolling resistance. Physical Review E 78, 021301.

Evans, A.G., Linzer, M., 1977. Acoustic emission in brittle materials. Annual Review of Materials Science 7, 179–208.

Fan, Y., Gu, F., Ball, A., 2010. Modelling acoustic emissions generated by sliding friction. Wear 268, 811–815.

Fernandes, F., Syahrial, A.I., Valdes, J.R., 2010. Monitoring the oedometric compression of sands with acoustic emissions. Geotechnical Testing Journal, American Society for Testing and Materials 33, 410–415.

Fisher, R.A., 1926. On the capillary forces in an ideal soil; correction of formulae given by W. B. Haines. Journal of Agricultural Science 16, 492–505.

Fortin, J., Stanchits, S., Dresen, G., Gueguen, Y., 2006. Acoustic emission and velocities associated with the formation of compaction bands in sandstone. Journal of Geophysical Research - Solid Earth 111, B10203.

Fournier, Z., Geromichalos, D., Herminghaus, S., Kohonen, M.M., Mugele, F., Scheel, M., Schulz, M., Schulz, B., Schier, C., Seemann, R., Skudelny, A., 2005. Mechanical properties of wet granular materials. Journal of Physics: Condensed Matter 17, S477.

Frank, F.C., Lawn, B.R., 1967. On the theory of Hertzian fracture. Proceedings of the Royal Society A 299, 291–306.

Garcimartin, A., Guarino, A., Bellon, L., Ciliberto, S., 1997. Statistical properties of fracture precursors. Physical Review Letters 79, 3202–3205.

Gardel, E., Seitaridou, E., Facto, K., Keene, E., Hattam, K., Easwar, N., Menon, N., 2009. Dynamical fluctuations in dense granular flows. Philosophical Transactions of the Royal Society A 367, 5109–5121.

Gardiner, B.S., Tordesillas, A., 2004. Micromechanics of shear bands. International Journal of Solids and Structures 41, 5885–5901.

Gardiner, B., Tordesillas, A., 2005. Micromechanical constitutive modelling of granular media: evolution and loss of contact in particle clusters. Journal of Engineering Mathematics 52, 93–106.

Gassmann, F., 1951. Elastic waves through a packing of spheres. Geophysics 16, 673–685.
Gauglitz, P., Radke, C., 1990. The dynamics of liquid film breakup in constricted cylindrical capillaries. Journal of Colloid and Interface Science 134, 14–40.
George, L.A., Dewoolkar, M.M., Znidarcic, D., 2009. Simultaneous laboratory measurement of acoustic and hydraulic properties of unsaturated soils. Vadose Zone Journal 8, 633–642.
Gilardi, G., Sharf, I., 2002. Literature survey of contact dynamics modelling. Mechanism and Machine Theory 37, 1213–1239.
Gilles, B., Coste, C., 2003. Low-frequency behavior of beads constrained on a lattice. Physical Review Letters 90, 174302.
Girard, L., Amitrano, D., Weiss, J., 2010. Failure as a critical phenomenon in a progressive damage model. Journal of Statistical Mechanics – Theory and Experiment 2010, P01013.
Goddard, J.D., 1990. Nonlinear elasticity and pressure-dependent wave speeds in granular media. Proceedings of the Royal Society A 430, 105–131.
Golchert, D., Moreno, R., Ghadiri, M., Litster, J., 2004. Effect of granule morphology on breakage behaviour during compression. Powder Technology 143–144, 84–96.
Goldhirsch, I., 2008. Introduction to granular temperature. Powder Technology 182, 130–136.
Goren, L., Aharonov, E., Sparks, D., Toussaint, R., 2010. Pore pressure evolution in deforming granular material: A general formulation and the infinitely stiff approximation. Journal of Geophysical Research 115, B09216.
Goren, L., Aharonov, E., Sparks, D., Toussaint, R., 2011. The mechanical coupling of fluid-filled granular material under shear. Pure and Applied Geophysics 168, 2289–2323.
Gray, D.H., Leiser, A.T., 1982. Biotechnical Slope Protection and Erosion Control. Van Nostrand Rheinhold, New York. 271 pp.
Grgic, D., Amitrano, D., 2009. Creep of a porous rock and associated acoustic emission under different hydrous conditions. Journal of Geophysical Research 114, B10201.
Griffiths, S., Rescaglio, A., Melo, F., 2010. Ultrasound propagation in wet and airless non-consolidated granular materials. Ultrasonics 50, 139–144.
Grof, Z., Lawrence, C.J., Stepanek, F., 2008. The strength of liquid bridges in random granular materials. Journal of Colloid and Interface Science 319, 182–192.
Grosse, C.E., Ohtsu, M., 2008. Acoustic Emission Testing. Springer, Berlin, Heidelberg. 396 pp.
Guarino, A., Garcimartin, A., Ciliberto, S., 1998. An experimental test of the critical behaviour of fracture precursors. European Physical Journal B 6, 13–24.
Guarino, A., Ciliberto, S., Garcimartin, A., Zei, M., Scorretti, R., 2002. Failure time and critical behaviour of fracture precursors in heterogeneous materials. European Physical Journal B 26, 141–151.
Guimaraes, M., Valdes, J., Palomino, A., Santamarina, J., 2007. Aggregate production: Fines generation during rock crushing. International Journal of Mineral Processing 81, 237–247.
Gutenberg, B., Richter, C., 1954. Seismicity of the Earth. Princeton Univ. Press. 131 pp.
Halasz, Z., Kun, F., 2009. Fiber bundle model with stick-slip dynamics. Physical Review E 80, 027102.
Hardin, B.O., 1965. The nature of damping in sands. Journal of the Soil Mechanics and Foundation Division 91, 63–98.
Hardy, C., Baronet, C.N., Tordion, G.V., 1971. The elasto-plastic indentation of a half-space by a rigid sphere. International Journal for Numerical Methods in Engineering 3, 451–462.
Hemmer, P.C., Hansen, A., 1992. The distribution of simultaneous fiber failures in fiber bundles. Journal of Applied Mechanics 59, 909–914.
Henrique, C., Aguirre, M., Calvo, A., Ippolito, I., Bideau, D., 1997. Experimental acoustic technique in granular flows. Powder Technology 94, 85–89.
Herminghaus, S., 2005. Dynamics of wet granular matter. Advances in Physics 54, 221–261.
Hertz, H., 1882. Über die Berührung fester elastischer Körper (On the contact of elastic solids). Journal für die Reine und Angewandte Mathematik 92, 156–171 For English translation see *Miscellaneous papers by H. Hertz. Eds. Jones and Schott. London. Macmillian. 1896*.
Heslot, F., Baumberger, T., Perrin, B., Caroli, B., Caroli, C., 1994. Creep, stick-slip, and dry-friction dynamics: Experiments and a heuristic model. Physical Review E 49, 4973–4988.
Hidalgo, R.C., Grosse, C.U., Kun, F., Reinhardt, H.W., Herrmann, H.J., 2002. Evolution of percolating force chains in compressed granular media. Physical Review Letters 89, 205501.
Hirata, T., 1987. Omori's power law aftershock sequences of microfracturing in rock fracture experiment. Journal of Geophysical Research - Solid Earth 92, 6215–6221.
Holmes, J.D., Carey, W.M., Dediu, S.M., Siegmann, W.L., 2007. Nonlinear frequency-dependent attenuation in sandy sediments. Journal of the Acoustical Society of America 121, EL218–EL222.
Holt, J., 1976. Electronic noise in acoustic emission measurements. Non-Destructive Testing 9, 66–70.
Huck, P.J., Koerner, R.M., 1981. Acoustic emission monitoring of soil and rock grouting. In: Drnevich, V.P., Gray, R.E. (Eds.), Acoustic Emission in Geotechnical Engineering Practice, ASTM STP 750. American Society for Testing and Materials, Philadelphia, pp. 155–163.
Hung, M.H., Lauchle, G.C., Wang, M.C., 2009. Seepage-induced acoustic emission in granular soils. Journal of Geotechnical and Geoenvironmental Engineering 135, 566–572.
Hunter, S., 1957. Energy absorbed by elastic waves during impact. Journal of the Mechanics and Physics of Solids 5, 162–171.
Hutchings, I.M., 1979. Energy absorbed by elastic waves during plastic impact. Journal of Physics D: Applied Physics 12, 1819.
Ibrahim, R.A., 1994a. Friction-induced vibration, chatter, squeal, and chaos. Part 1: Mechanics of contact and friction. Applied Mechanics Reviews 47, 209–226.
Ibrahim, R.A., 1994b. Friction-induced vibration, chatter, squeal, and chaos. Part 2: Dynamics and modeling. Applied Mechanics Reviews 47, 227–253.
Inaudi, D., Glisic, B., 2005. Application of distributed fiber optic sensory for SHM. 2nd International Conference on Structural Health Monitoring of Intelligent Infrastructure, Shenzhen, China, pp. 1–7.
Ismail, M.A., Joer, H.A., Sim, W.H., Randolph, M.F., 2002. Effect of cement type on shear behavior of cemented calcareous soil. Journal of Geotechnical and Geoenvironmental Engineering 128, 520–529.
Iten, M., 2008. Landslide monitoring using a road-embedded optical fiber sensor. Proceedings of SPIE 6933, 693315.
Iten, M., 2011. Distributed fiber optic sensor development, testing, and evaluation for geotechnical monitoring applications. Proceedings of SPIE 7982, 798207.
Jackson, D.D., Anderson, D.L., 1970. Physical mechanisms of seismic-wave attenuation. Reviews of Geophysics 8, 1–63.
Jarzynski, J., Hughes, R., Hickman, T.R., A., B.J., 1981. Frequency response of interferometric fiber-optic coil hydrophones. Journal of the Acoustical Society of America 69, 1799–1808.
Jia, X., 2004. Codalike multiple scattering of elastic waves in dense granular media. Physical Review Letters 93, 154303.
Jia, X., Caroli, C., Velicky, B., 1999. Ultrasound propagation in externally stressed granular media. Physical Review Letters 82, 1863–1866.
Jia, X., Brunet, T., Laurent, J., 2011. Elastic weakening of a dense granular pack by acoustic fluidization: Slipping, compaction, and aging. Physical Review E 84, 020301.
Jiaa, C., Dornfeld, D., 1990. Experimental studies of sliding friction and wear via acoustic emission signal analysis. Wear 139, 403–424.
Jiang, X.J., Wang, J.D., Jiang, B.B., Yang, Y., Hou, L.X., 2007. Study of the power spectrum of acoustic emission (AE) by accelerometers in fluidized beds. Industrial and Engineering Chemistry Research, American Chemical Society 46, 6904–6909.
Jin, A., Aki, K., 1986. Temporal change in coda Q before the Tangshan earthquake of 1976 and the Haicheng earthquake of 1975. Journal of Geophysical Research 91, 665–673.
Job, S., Melo, F., Sokolow, A., Sen, S., 2005. How Hertzian solitary waves interact with boundaries in a 1d granular medium. Physical Review Letters 94, 178002.
Job, S., Santibanez, F., Tapia, F., Melo, F., 2008. Nonlinear waves in dry and wet Hertzian granular chains. Ultrasonics 48, 506–514.
Johansen, A., Sornette, D., 2000. Critical ruptures. European Physical Journal B 18, 163–181.
Johnson, K.L., 1985. Contact Mechanics. Cambridge University Press, Cambridge. 468 pp.
Johnston, D.H., Toksoz, M.N., Timur, A., 1979. Attenuation of seismic waves in dry and saturated rocks: II. Mechanisms. Geophysics 44, 691–711.
Kageyama, K., Murayama, H., Ohsawa, I., Kanai, M., Nagata, K., Machijima, Y., Matsumura, F., 2005. Acoustic emission monitoring of a reinforced concrete structure by applying new fiber-optic sensors. Smart Materials and Structures 14, S52.
Kanamori, H., Given, J.W., 1981. Use of long-period surface waves for rapid determination of earthquake-source parameters. Physics of the Earth and Planetary Interiors 27, 8–31.
Karner, S.L., Chester, F.M., Kronenberg, A.K., Chester, J.S., 2003. Subcritical compaction and yielding of granular quartz sand. Tectonophysics 377, 357–381.
Kino, G.S., 1987. Acoustic Waves: Devices, Imaging, and Analog Signal Processing. Prentice-Hall Signal Processing SeriesPrentice-Hall, New Jersey.
Knopoff, L., 1964. Q. Reviews of Geophysics 2, 625–660.
Koerner, R., Lord, A., McCabe, W., Curran, J., 1976. Acoustic-emission behavior of granular soils. Journal of the Geotechnical Engineering Division – ASCE 103, 1460–1461.
Koerner, R.M., Lord, A.E., McCabe, W.M., 1977. Acoustic-emission behavior of cohesive soils. Journal of the Geotechnical Engineering Division – ASCE 103, 837–850.
Koerner, R.M., McCabe, W.M., Lord, A.E., 1981a. Overview of acoustic emission monitoring of rock structures. Rock Mechanics and Rock Engineering 14, 27–35.
Koerner, R.M., Mccabe, W.M., Lord, A., 1981b. Acoustic emission behavior and monitoring of soil. In: Drnevich, V.P., Gray, R.E. (Eds.), Acoustic Emission in Geotechnical Engineering Practice, ASTM STP 750. American Society for Testing and Materials, Philadelphia, pp. 93–141.
Kogut, L., Komvopoulos, K., 2004. Analysis of the spherical indentation cycle for elastic perfectly plastic solids. Journal of Materials Research 19, 3641–3653.
Kohler, N., Spies, T., Dahm, T., 2009. Seismicity patterns and variation of the frequency-magnitude distribution of microcracks in salt. Geophysical Journal International 179, 489–499.
Kun, F., Hidalgo, R., Raischel, F., Herrmann, H., 2006. Extension of fibre bundle models for creep rupture and interface failure. International Journal of Fracture 140, 255–265.
Labuz, J.F., Cattaneo, S., Chen, L.H., 2001. Acoustic emission at failure in quasi-brittle materials. Construction and Building Materials 15, 225–233.
Landau, L.D., Lifshitz, E.M., 1986. Theory of Elasticity, 3rd edition. Pergamon Press, Oxford, New York, Beijing, Frankfurt, Sao Paulo, Sidney, Tokyo, Toronto. 334 pp.
Lavrov, A., Shkuratnik, V., 2005. Deformation-and fracture-induced acoustic emission in rocks. Acoustical Physics 51, S2–S11.
Lee, J.S., Santamarina, J.C., 2005. Bender elements: Performance and signal interpretation. Journal of Geotechnical and Geoenvironmental Engineering 131, 1063–1070.
Lee, K.I., Humphrey, V.F., Kim, B.N., Yoon, S.W., 2007. Frequency dependencies of phase velocity and attenuation coefficient in a water-saturated sandy sediment from 0.3 to 1.0 MHz. Journal of the Acoustical Society of America 121, 2553–2558.
Leong, E.C., Yeo, S.H., Rahardjo, H., 2004. Measurement of wave velocities and attenuation using an ultrasonic test system. Canadian Geotechnical Journal 41, 844–860.
Levine, D., 2001. Jamming and the Statistics of Granular Materials. In: Liu, Andrea, Nagel, Sidney (Eds.), Jamming and Rheology. Taylor & Francis, London and New York, pp. 9–19.

Li, Y., Aydin, A., 2010. Behavior of rounded granular materials in direct shear: Mechanisms and quantification of fluctuations. Engineering Geology 115, 96–104.
Li, F., Murayama, H., Kageyama, K., Ohsawa, I., 2009. Multiple damage assessment in composite laminates using a Doppler-effect-based fiber-optic sensor. Measurement Science and Technology 20, 115109.
Liakopoulou Morris, F., Main, I.G., Crawford, B.R., Smart, B.G.D., 1994. Microseismic properties of a homogeneous sandstone during fault nucleation and frictional sliding. Geophysical Journal International 119, 219–230.
Liu, C.h., 1994. Spatial patterns of sound propagation in sand. Physical Review B 50, 782–794.
Liu, C.h., Nagel, S.R., 1992. Sound in sand. Physical Review Letters 68, 2301–2304.
Liu, C.h., Nagel, S.R., 1993. Sound in a granular material: Disorder and nonlinearity. Physical Review B 48, 15646–15650.
Liu, C.H., Nagel, S.R., Schecter, D.A., Coppersmith, S.N., Majmudar, S., Narayan, O., Witten, T.A., 1995. Force fluctuations in bead packs. Science 269, 513–515.
Lo, W., Sposito, G., Majer, E., 2005. Wave propagation through elastic porous media containing two immiscible fluids. Water Resources Research 41.
Lockner, D., 1993. The role of acoustic emission in the study of rock fracture. International Journal of Rock Mechanics and Mining Sciences & Geomechanics Abstracts 30, 883–899.
Longhi, E., Easwar, N., Menon, N., 2002. Large force fluctuations in a flowing granular medium. Physical Review Letters 89, 045501.
Lord, A.E., Koerner, R.M., 1974. Acoustic-emission response of dry soils. Journal of Testing and Evaluation 2, 159–162.
Lord, A.E., Koerner, R.M., 1975. Acoustic emissions in soils and their use in assessing earth dam stability. Journal of the Acoustical Society of America 57, 516–519.
Lorenceau, E., Quere, D., Ollitrault, J.Y., Clanet, C., 2002. Gravitational oscillations of a liquid column in a pipe. Physics of Fluids 14, 1985–1992.
Løvoll, G., Måløy, K.J., Flekkøy, E.G., 1999. Force measurements on static granular materials. Physical Review E 60, 5872–5878.
Lu, Z., Sabatier, J.M., 2009. Effects of soil water potential and moisture content on sound speed. Soil Science Society of America Journal 73, 1614–1625.
Maaskant, R., Alavie, T., Measures, R.M., Tadros, G., Rizkalla, S.H., Guha-Thakurta, A., 1997. Fiber-optic bragg grating sensors for bridge monitoring. Cement and Concrete Composites 19, 21–33.
Main, I.G., Meredith, P.G., Jones, C., 1989. A reinterpretation of the precursory seismic b-value anomaly from fracture mechanics. Geophysical Journal International 96, 131–138.
Mair, K., Marone, C., Young, R.P., 2007. Rate dependence of acoustic emissions generated during shear of simulated fault gouge. Bulletin of the Seismological Society of America 97, 1841–1849.
Majmudar, T.S., Behringer, R.P., 2005. Contact force measurements and stress-induced anisotropy in granular materials. Nature 435, 1079–1082.
Mason, G., Clark, W., 1968. Tensile strength of wet granular materials. Nature 219, 149–150.
Mavko, G.M., Nur, A., 1979. Wave attenuation in partially saturated rocks. Geophysics 44, 161–178.
Mayr, S.I., Stanchits, S., Langenbruch, C., Dresen, G., Shapiro, S.A., 2011. Acoustic emission induced by pore-pressure changes in sandstone samples. Geophysics 76, MA21–MA32.
McClung, D., 1986. Mechanics of snow slab failure from a geotechnical perspective. Proc. Davos Symposium, Davos, Switzerland, pp. 475–508.
McLaskey, G.C., Glaser, S.D., 2011. Micromechanics of asperity rupture during laboratory stick slip experiments. Geophysical Research Letters 38, L12302.
Measures, R.M., 2001. Structural Monitoring With Fiber Optic Technology. Academic Press, San Diego, San Francisco, New York, Boston, London, Sidney, Tokyo. 761 pp.
Mindlin, R.D., Deresiewicz, H., 1953. Elastic spheres in contact under varying oblique forces. Journal of Applied Mechanics 75, 327–344.
Mitarai, N., Nori, F., 2006. Wet granular materials. Advances in Physics 55, 1–45.
Mlakar, V., Hassani, F., Momayez, M., 1993. Crack development and acoustic emission in potash rock. International Journal of Rock Mechanics and Mining Sciences & Geomechanics Abstracts 30, 305–319.
Mogi, K., 1962. Magnitude frequency relation for elastic shocks accompanying fractures of various materials and some related problems in earthquakes. Bulletin of the Earthquake Research Institute 40, 831–853.
Mollot, D.J., Tsamopoulos, J., Chen, T.Y., Ashgriz, N., 1993. Nonlinear dynamics of capillary bridges: Experiments. Journal of Fluid Mechanics 255, 411–435.
Mueth, D.M., Jaeger, H.M., Nagel, S.R., 1998. Force distribution in a granular medium. Physical Review E 57, 3164–3169.
Mueth, D.M., Debregeas, G.F., Karczmar, G.S., Eng, P.J., Nagel, S.R., Jaeger, H.M., 2000. Signatures of granular microstructure in dense shear flows. Nature 406, 385–389.
Mühlhaus, H.B., Vardoulakis, I., 1987. The thickness of shear bands in granular materials. Geotechnique 37, 271–283.
Nyborg, W.L., Rudnick, I., Schilling, H.K., 1950. Experiments on acoustic absorption in sand and soil. Journal of the Acoustical Society of America 22, 422–425.
Oelze, M.L., O'Brien, W.D., Darmody, R.G., 2002. Measurement of attenuation and speed of sound in soils. Soil Science Society of America Journal 66, 788–796.
Ohtsu, M., Watanabe, H., 2001. Quantitative damage estimation of concrete by acoustic emission. Construction and Building Materials 15, 217–224.
Or, D., Smets, B., Wraith, J., Dechesne, A., Friedman, S., 2007. Physical constraints affecting bacterial habitats and activity in unsaturated porous media - a review. Advances in Water Resources 30, 1505–1527.
Ord, A., Hobbs, B., Regenauer-Lieb, K., 2007. Shear band emergence in granular materials – a numerical study. International Journal for Numerical and Analytical Methods in Geomechanics 31, 373–393.
Othonos, A., 1997. Fiber bragg gratings. The Review of Scientific Instruments 68, 4309–4341.
Palmer, A.C., Rice, J.R., 1973. The growth of slip surfaces in the progressive failure of over-consolidated clay. Proceedings of the Royal Society A 332, 527–548.
Paparo, G., Gregori, G., Coppa, U., De Ritis, R., Taloni, A., 2002. Acoustic emission (AE) as a diagnostic tool in geophysics. Annals of Geophysics 45, 401–416.
Patitsas, A.J., 2010. Squeal vibrations, glass sounds, and the stick-slip effect. Canadian Journal of Physics 88, 863–876.
Pierrat, P., Caram, H.S., 1997. Tensile strength of wet granular materials. Powder Technology 91, 83–93.
Pitois, O., Moucheront, P., Chateau, X., 2001. Rupture energy of a pendular liquid bridge. European Physical Journal B 23, 79–86.
Pohlman, N.A., Severson, B.L., Ottino, J.M., Lueptow, R.M., 2006. Surface roughness effects in granular matter: Influence on angle of repose and the absence of segregation. Physical Review E 73, 031304.
Pradhan, S., Hemmer, P.C., 2008. Energy bursts in fiber bundle models of composite materials. Physical Review E 77, 031138.
Pradhan, S., Hemmer, P.C., 2011. Prediction of the collapse point of overloaded materials by monitoring energy emissions. Physical Review E 83, 041116.
Pradhan, S., Hansen, A., Hemmer, P.C., 2006. Crossover behavior in failure avalanches. Physical Review E 74, 016122.
Pradhan, S., Hansen, A., Chakrabarti, B.K., 2010. Failure processes in elastic fiber bundles. Reviews of Modern Physics 82, 499.
Pride, S.R., Toussaint, R., 2002. Thermodynamics of fiber bundles. Physica A: Statistical Mechanics and its Applications 312, 159–171.
Radjai, F., Evesque, P., Bideau, D., Roux, S., 1995. Stick-slip dynamics of a one-dimensional array of particles. Physical Review E 52, 5555–5564.
Radjai, F., Jean, M., Moreau, J.J., Roux, S., 1996. Force distributions in dense two-dimensional granular systems. Physical Review Letters 77, 274–277.
Radjai, F., Wolf, D.E., Jean, M., Moreau, J.J., 1998. Bimodal character of stress transmission in granular packings. Physical Review Letters 80, 61–64.
Raischel, F., Kun, F., Herrmann, H.J., 2006a. Failure process of a bundle of plastic fibers. Physical Review E 73, 066101.
Raischel, F., Kun, F., Hidalgo, R.C., Herrmann, H.J., 2006b. Statistical Damage Models: Fiber Bundle Models. In: Busse, G., Kroeplin, B.H., Wittel, F.K. (Eds.), Damage and its Evolution in Fiber-Composite Materials: Simulation and Non-Destructive Evaluation. Universität Stuttgart, Stuttgart, pp. 443–471.
Read, H., Hegemier, G., 1984. Strain softening of rock, soil and concrete – a review article. Mechanics of Materials 3, 271–294.
Read, M.D., Ayling, M.R., Meredith, P.G., Murrell, S.A.F., 1995. Microcracking during triaxial deformation of porous rocks monitored by changes in rock physical properties - 2: Pore volumometry and acoustic emission measurements on water-saturated rocks. Tectonophysics 245, 223–235.
Rechenmacher, A., Abedi, S., Chupin, O., 2010. Evolution of force chains in shear bands in sands. Geotechnique 60, 343–351.
Reiweger, I., Schweizer, J., Dual, J., Herrmann, H.J., 2009. Modelling snow failure with a fibre bundle model. Journal of Glaciology 55, 997–1002.
Rice, J.R., 1968. A path independent integral and approximate analysis of strain concentration by notches and cracks. Journal of Applied Mechanics 35, 379–386.
Rice, J.R., Lapusta, N., Ranjith, K., 2001. Rate and state dependent friction and the stability of sliding between elastically deformable solids. Journal of the Mechanics and Physics of Solids 49, 1865–1898.
Richefeu, V., El Youssoufi, M., Radjai, F., 2006. Shear strength properties of wet granular materials. Physical Review E 73, 051304.
Rioual, F., Valance, A., Bideau, D., 2000. Experimental study of the collision process of a grain on a two-dimensional granular bed. Physical Review E 62, 2450–2459.
Rosti, J., Koivisto, J., Alava, M.J., 2010. Statistics of acoustic emission in paper fracture: precursors and criticality. Journal of Statistical Mechanics – Theory and Experiment P02016.
Rouse, C., Styles, P., Wilson, S., 1991. Microseismic emissions from flowslide-type movements in south wales. Engineering Geology 31, 91–110.
Salminen, L.I., Tolvanen, A.I., Alava, M.J., 2002. Acoustic emission from paper fracture. Physical Review Letters 89, 185503.
Sammonds, P., Ohnaka, M., 1998. Evolution of microseismicity during frictional sliding. Geophysical Research Letters 25, 699–702.
Savage, J.C., 1965. Attenuation of elastic waves in granular mediums. Journal of Geophysical Research 70, 3935–3942.
Scheel, M., Seemann, R., Brinkmann, M., Di Michiel, M., Sheppard, A., Breidenbach, B., Herminghaus, S., 2008. Morphological clues to wet granular pile stability. Nature Materials 7, 189–193.
Scholz, H., 1968. The frequency-magnitude relation of microfracturing in rock and its relation to earthquakes. Bulletin of the Seismological Society of America 58, 399–415.
Schubnel, A., Thompson, B.D., Fortin, J., Guguen, Y., Young, R.P., 2007. Fluid-induced rupture experiment on fontainebleau sandstone: Premonitory activity, rupture propagation, and aftershocks. Geophysical Research Letters 34, L19307.
Schwarz, M., Cohen, D., Or, D., 2010. Root-soil mechanical interactions during pullout and failure of root bundles. Journal of Geophysical Research 115, F04035.
Scruby, C.B., 1987. An introduction to acoustic emission. Journal of Physics E: Scientific Instruments 20, 946.
Selker, J.S., Thvenaz, L., Huwald, H., Mallet, A., Luxemburg, W., van de Giesen, N., Stejskal, M., Zeman, J., Westhoff, M., Parlange, M.B., 2006. Distributed fiber-optic temperature sensing for hydrologic systems. Water Resources Research 42, W12202.
Senfaute, G., Duperret, A., Lawrence, J.A., 2009. Micro-seismic precursory cracks prior to rock-fall on coastal chalk cliffs: A case study at Mesnil-Val, Normandie, NW France. Natural Hazards and Earth System Sciences 9, 1625–1641.
Sethna, J.P., Dahmen, K.A., Myers, C.R., 2001. Crackling noise. Nature 410, 242–250.

Shigeishi, M., Colombo, S., Broughton, K.J., Rutledge, H., Batchelor, A.J., Forde, M.C., 2001. Acoustic emission to assess and monitor the integrity of bridges. Construction and Building Materials 15, 35–49.
Shiotani, T., 2006. Evaluation of long-term stability for rock slope by means of acoustic emission technique. NDT&E International 39, 217–228.
Shiotani, T., Ohtsu, M., 1999. Prediction of slope failure based on ae activity. In: Vahaviolos, S. (Ed.), Acoustic Emission: Standards And Technology Update. American Society Testing And Materials, West Conshohocken, pp. 156–172.
Simons, S.J.R., Fairbrother, R.J., 2000. Direct observations of liquid binder-particle interactions: The role of wetting behaviour in agglomerate growth. Powder Technology 110, 44–58.
Smith, R.L., Phoenix, S.L., 1981. Asymptotic distributions for the failure of fibrous materials under series-parallel structure and equal load-sharing. Journal of Applied Mechanics 48, 75–82.
Somfai, E., Roux, J.N., Snoeijer, J.H., van Hecke, M., van Saarloos, W., 2005. Elastic wave propagation in confined granular systems. Physical Review E 72, 021301.
Sommerfeld, R.A., Gubler, H., 1983. Snow avalanches and acoustic emissions. Annals of Glaciology 4, 271–276.
Spillmann, T., Maurer, H., Green, A.G., Heincke, B., Willenberg, H., Husen, S., 2007. Microseismic investigation of an unstable mountain slope in the Swiss Alps. Journal of Geophysical Research 112, B07301.
Stanchits, S., Fortin, J., Gueguen, Y., Dresen, G., 2009. Initiation and propagation of compaction bands in dry and wet Bentheim sandstone. Pure and Applied Geophysics 166, 843–868.
Staron, L., Radjai, F., Vilotte, J.P., 2006. Granular micro-structure and avalanche precursors. Journal of Statistical Mechanics P07014.
Staszewski, W.J., Boller, C., Tomlinson, G.R., 2004. Health Monitoring of Aerospace Structures: Smart Sensor Technologies and Signal Processing. John Wiley & Sons, Ltd., Chichester, UK. 266 pp.
Stoll, R.D., 1979. Experimental studies of attenuation in sediments. Journal of the Acoustical Society of America 66, 1152–1160.
Stump, B.W., Johnson, L.R., 1977. The determination of source properties by the linear inversion of seismograms. Bulletin of the Seismological Society of America 67, 1489–1502.
Swindlehurst, W., 1973. Acoustic emission - 1 Introduction. Non-Destructive Testing 6, 152–158.
Tanimoto, K., Nakamura, J., 1981. Studies of acoustic emission in soil. In: Drnevich, V.P., Gray, R.E. (Eds.), Acoustic Emission in Geotechnical Engineering Practice, ASTM STP 750. American Society for Testing and Materials, pp. 164–173.
Thornton, C., 2000. Numerical simulations of deviatoric shear deformation of granular media. Geotechnique 50, 43–53.
Tisdall, J.M., Oades, J.M., 1982. Organic matter and water-stable aggregates in soils. Journal of Soil Science 33, 141–163.
Tordesillas, A., 2007. Force chain buckling, unjamming transitions and shear banding in dense granular assemblies. Philosophical Magazine 87, 4987–5016.
Tordesillas, A., Behringer, R.P., 2009. Are we there yet? following the energy trail in cohesionless granular solids. In: Kolymbas, D., Viggiani, G. (Eds.), Mechanics of Natural Solids. Springer, Berlin, Heidelberg, pp. 47–83.
Tordesillas, A., Muthuswamy, M., 2009. On the modeling of confined buckling of force chains. Journal of the Mechanics and Physics of Solids 57, 706–727.
Tournat, V., Gusev, V.E., 2009. Nonlinear effects for coda-type elastic waves in stressed granular media. Physical Review E 80, 011306.
Tournat, V., Castagnde, B., Gusev, V., Bquin, P., 2003. Self-demodulation acoustic signatures for nonlinear propagation in glass beads. Comptes Rendus Mecanique 331, 119–125.
Tournat, V., Gusev, V.E., Castagnde, B., 2004. Subharmonics and noise excitation in transmission of acoustic wave through unconsolidated granular medium. Physics Letters A 326, 340–348.
Toussaint, R., Pride, S.R., 2002a. Fracture of disordered solids in compression as a critical phenomenon. I. Statistical mechanics formalism. Physical Review E 66, 036135.
Toussaint, R., Pride, S.R., 2002b. Fracture of disordered solids in compression as a critical phenomenon. II. Model hamiltonian for a population of interacting cracks. Physical Review E 66, 036136.
Toussaint, R., Pride, S.R., 2002c. Fracture of disordered solids in compression as a critical phenomenon. III. Analysis of the localization transition. Physical Review E 66, 036137.
Toussaint, R., Pride, S.R., 2005. Interacting damage models mapped onto ising and percolation models. Physical Review E 71, 046127.
Turcotte, D.L., Newman, W.I., Shcherbakov, R., 2003. Micro and macroscopic models of rock fracture. Geophysical Journal International 152, 718–728.
Tyree, M.T., Sperry, J.S., 1989. Characterization and propagation of acoustic emission signals in woody plants: Towards an improved acoustic emission counter. Plant, Cell & Environment 12, 371–382.
van Herwijnen, A., Schweizer, J., 2011a. Monitoring avalanche activity using a seismic sensor. Cold Regions Science and Technology 69, 165–176.
van Herwijnen, A., Schweizer, J., 2011b. Seismic senosor array for monitoring an avalanche start zone: design, deployment and preliminary results. Journal of Glaciology 57, 267–276.
Vanel, L., Ciliberto, S., Cortet, P.P., Santucci, S., 2009. Time-dependent rupture and slow crack growth: Elastic and viscoplastic dynamics. Journal of Physics D: Applied Physics 42, 214007.
Velea, D., Shields, F.D., Sabatier, J.M., 2000. Elastic wave velocities in partially saturated Ottawa sand: Experimental results and modeling. Soil Science Society of America Journal 64, 1226–1234.
Villet, W., Mitchell, J., Tringale, P., 1981. Acoustic emissions generated during the quasi-static cone penetration of soils. In: Drnevich, V.P., Gray, R.E. (Eds.), Acoustic Emission in Geotechnical Engineering Practice, ASTM STP 750. American Society for Testing and Materials, pp. 175–193.
von Seggern, D., 1980. A random stress model for seismicity statistics and earthquake prediction. Geophysical Research Letters 7, 637–640.
Wang, Y.H., Santamarina, J., 2007. Attenuation in sand: an exploratory study on the small-strain behavior and the influence of moisture condensation. Granular Matter 9, 365–376.
Wang, B.J., Li, K., Shi, B., Wei, G.Q., 2009a. Test on application of distributed fiber optic sensing technique into soil slope monitoring. Landslides 6, 61–68.
Wang, Y., Ma, C., Yan, W., 2009b. Characterizing bond breakages in cemented sands using a mems accelerometer. Geotechnical Testing Journal 32, 1–10.
Warren, N.W., Latham, G.V., 1970. An experimental study of thermally induced microfracturing and its relation to volcanic seismicity. Journal of Geophysical Research 75, 4455–4464.
Weeks, J., Lockner, D., Byerlee, J., 1978. Change in b-values during movement on cut surfaces in granite. Bulletin of the Seismological Society of America 68, 333–341.
Welker, P., McNamara, S., 2011. Precursors of failure and weakening in a biaxial test. Granular Matter 13, 93–105.
Wilshaw, T.R., 1971. The Hertzian fracture test. Journal of Physics D: Applied Physics 4, 1567.
Wolf, D.E., Radjai, F., Dippel, S., 1998. Dissipation in granular materials. Philosophical Magazine 77, 1413–1425.
Yabe, Y., 2002. Rate dependence of ae activity during frictional sliding. Geophysical Research Letters 29, 1388.
Yabe, Y., 2008. Evolution of source characteristics of ae events during frictional sliding. Earth, Planets and Space 60, e5–e8.
Yabe, Y., Kato, N., Yamamoto, K., Hirasawa, T., 2003. Effect of sliding rate on the activity of acoustic emission during stable sliding. Pure and Applied Geophysics 160, 1163–1189.
Yamada, I., Masuda, K., Mizutani, H., 1989. Electromagnetic and acoustic emission associated with rock fracture. Physics of the Earth and Planetary Interiors 57, 157–168.
Young, P., Martin, C., 1993. Potential role of acoustic emission/microseismicity investigations in the site characterization and performance monitoring of nuclear waste repositories. International Journal of Rock Mechanics and Mining Sciences & Geomechanics Abstracts 30, 797–803.
Zaitsev, S., 1992. Robin Hood as self-organized criticality. Physica A: Statistical Mechanics and its Applications 189, 411–416.
Zang, A., Wagner, C.F., Dresen, G., 1996. Acoustic emission, microstructure, and damage model of dry and wet sandstone stressed to failure. Journal of Geophysical Research 101, 17507–17521.
Zang, A., Christian Wagner, F., Stanchits, S., Dresen, G., Andresen, R., Haidekker, M.A., 1998. Source analysis of acoustic emissions in Aue granite cores under symmetric and asymmetric compressive loads. Geophysical Journal International 135, 1113–1130.
Zeni, L., 2009. Optical fiber distributed sensors: A tool for in-situ structural and environmental monitoring. Italian Workshop on Landslides 2009, Rainfall Induced Landslides, Naples.
Zhang, J., Wong, T.F., Davis, D.M., 1990. Micromechanics of pressure-induced grain crushing in porous rocks. Journal of Geophysical Research 95, 341–352.
Zhang, X., Padgett, R.S., Basaran, O.A., 1996. Nonlinear deformation and breakup of stretching liquid bridges. Journal of Fluid Mechanics 329, 207–245.
Zhang, D., Shi, B., Cui, H.L., Xu, H., 2004. Improvement of spatial resolution of brillouin optical time domain reflectometer using spectral decomposition. Optica Applicata 34, 291–301.
Zhao, Z., Liu, C., Brogliato, B., 2008. Energy dissipation and dispersion effects in granular media. Physical Review E 78, 031307.
Zigone, D., Voisin, C., Larose, E., Renard, F., Campillo, M., 2011. Slip acceleration generates seismic tremor like signals in friction experiments. Geophysical Research Letters 38, L01315.
Zweifel, R., Zeugin, F., 2008. Ultrasonic acoustic emissions in drought-stressed trees – more than signals from cavitation? New Phytologist 179, 1070–1079.